**Republic of Iraq**
**Ministry of Higher Education and Scientific Research**
**University of Babylon**
**College of Engineering**

# *Enhancing Signal Detection in Non Orthogonal Multiple Access (NOMA) Communication Systems Through Deep Learning*

***A Thesis***
***Submitted to the Department of Electrical Engineering / College of Engineering / University of Babylon in Partial Fulfillment***
***of the Requirements for the Degree of Master in Engineering/ Electrical Engineering/ Communications.***

**By**
*Mohammed Najih Khadum Hamza*

**Supervised by**

*Prof. Dr. Raed Salem Hashim*

2023 A.D. 1445 A.H.

بِسْمِ اللَّـهِ الرَّحْمَـٰنِ الرَّحِيمِ

﴿يَرْفَعِ اللَّهُ الَّذِينَ آمَنـــــوُا مِنكُمْ
وَالَّذِينَ أُوتُـــــوا الْعِلْمَ دَرَجَاتٍ﴾

صدق الله العظيم

سورة المجادلة : 11

# *Supervisors Certification*

I certify that this thesis titled **"Enhancing Signal Detection in Non Orthogonal Multiple Access (NOMA) Communication Systems Through Deep Learning"** was prepared by **Mohammed Najih Khadum** under my supervision at the Electrical Engineering Department, College of Engineering at University of Babylon, in a partial fulfillment of the requirements for the degree of Master of Science in Electrical Engineering/Communication.

***Supervisor***

**Signature:**

**Name*: prof. Dr. Raed Salem Hashim***

**Date: / / 2023**

In view of the available recommendation, we forward this thesis for debate by the examining committee.

Head of the Electrical Engineering Department

**Signature:**

**Name: Prof .Dr. Qais Kareem Omran**

**Date: / / 2023**

# *Examining committee certificate*

We certify that we have read this thesis entitled **"Enhancing Signal Detection in Non Orthogonal Multiple Access (NOMA) Communication Systems Through Deep Learning"** and as an examining committee, examined the student **Mohammed Najih Khadum** in its content and that in our opinion it meets standard of a thesis for the degree of master in engineering/electrical engineering /Communication.

Signature:
Name: **Prof**
**Dr.Ehab A. Hussein**
(chairman)
Date: / / 2023

Signature:
Name: **Asst.Prof**
**Dr.Mustafa Rashid Ismael**
(member)
Date: / / 2023

Signature:
Name: **Asst.Prof**
**Dr.Hamza Mohammed Ridha Yahya**
(member)
Date: / / 2023

Signature:
Name: **Prof**
**Dr.Raed Salem Hashim**
(supervisor)
Date: / / 2023

Signature:
Name: **Prof. Dr.Qais Kareem Omran**
(Head of the Electrical Engineering Department)
Date: / / 2023

Signature:
Name: **Prof.Dr.Laith Ali Abdul - Rahaim**
(Dean of College of Engineering)
Date: / / 2023

# *Acknowledgements*

*Thanks be to God for the insight that inspired me, and praise be to Him for the blessings He has bestowed upon me, and to Him is the credit for achieving what I aspire to in this research. Praise be to God, who by His praise opens every book and by His remembrance every speech is issued, and by His praise the people of blessings enjoy the abode of reward.*

*It gives me great pleasure to extend my thanks and gratitude to* ***((prof. Dr.Raed Salem Hashim and Assistant. prof. Dr. Hilal Al-Libawy)****, they provided me with the information I needed in my research.*

*and for the great efforts he made for me since he proposed the subject of the research and his continuous supervision, and for his advice that helped me a lot in overcoming the difficulties I faced, calling from God success and brilliance in the scientific career.*

*I would like to extend my thanks and gratitude to the Deanship of the College of Engineering and the Presidency of the Electrical Engineering Department for the facilities and administrative procedures they provided me, which effectively contributed to the completion of the requirements of this research.*

.

**Researcher**

# Dedication

*To my wonderful father....* *who taught me the meaning of life and how to choose the best.*

*To my dear mother...* *the source of love and giving that words cannot describe, and my inspiration and encouragement in my scientific career*

*To my brothers and sister...* *my support and I share my joys and sorrows.*

*To my beloved wife…* *who supported me and endured many life's difficulties to complete my thesis.*

*To all my friends and to all those from whom I received advice and support;*

*I dedicate to you the summary of my scientific effort.*

# Abstract

Next-generation wireless communication seeks to outperform Orthogonal Multiple Access (OMA) in efficiency and users support. Non-Orthogonal Multiple Access (NOMA) shines in this regard, allowing numerous users and services access to all subcarriers without orthogonality constraints. However, as number of users increase  can hinder energy efficiency. Hybrid OFDM-NOMA system offer a powerful approach to address this challenges and significantly improve spectral efficiency, where transmits multiple user packets as a single signal, demanding advanced receiver algorithms like Successive Interference Cancellation (SIC). SIC-based techniques require perfect tracking of channel state by some channel estimation mechanism.Imperfect channel estimation, affecting SIC reliability.

To tackle this challenge effectively, an exciting avenue involves harnessing the capabilities of Deep Learning (DL) algorithms for rapid signal detection and channel estimation in one-shot scenarios.This thesis proposes two new DL approaches for enhancing hybrid (OFDM-NOMA) signal detection.The first approach is the Gated Recurrent Units (GRU) algorithm. GRU has two gates (update and reset), improving performance by addressing time dependence and gradients in Recurrent Neural Networks (RNN).

The second proposed system is the One-Dimensional Convolutional Neural Networks (1-dCNN). This approach addresses the limitations of current DL methods by using a 1-dimensional convolution layer for feature extraction instead of relying on time dependencies for data classification.

Through several testing, the GRU layer was adjusted to a size of 64, while the proposed (1-dCNN) adjusted with two sets of convolutional layers. Each set consisted of 32 filters with a size of 3 and a stride of 2. These parameter choices were made based on extensive experimentation and analysis, with the primary

objective of achieving consistent generalization potential and mitigating overfitting .The proposed GRU demonstrates superior performance in terms of Signal to Noise Ratio (SNR). GRU outperforms Long-Short Term Memory LSTM by 2dB and overcome Bi-Directional LSTM (BILSTM) by 4dB. Moreover, the proposed GRU outperforms traditional methods such as Least Squared Error (LS),Mean Sequared Error (MMSE) and Maximum Liklihode ( ML) for channel estimation.

Additionally, the proposed 1-dCNN outperforms GRU by 4dB. Both the GRU and 1-d CNN approaches were tested under various scenarios by adjusting parameters such as cyclic prefix (CP), pilot subcarrier and increasing the number of paths. In all different conditions, both approaches consistently outperform the state-of-the-art methods in literature review , with 1-dCNN particularly overcome GRU. This thesis examines training times of various neural network architectures, including 1-dCNN, GRU, LSTM, and BiLSTM, on a computer equipped with an Intel Core i5-7210M CPU @ 2.50GHz, 2 cores, and an external NVidia GeForce 630 GPU with 2GB memory. The results demonstrate that both GRU and 1-dCNN outperform LSTM and BiLSTM, with 1-dCNN training approximately 4 minutes faster than GRU.

# List of Contents

# List of Contents

# List of Tables

# List of Figures

# List of Figures

# List of Abbreviations

| Abbreviation | Definition |
|---|---|
| Adam | Adaptive gradient descent methods |
| BILSTM | Bi-directional long short-term memory |
| BS | Base station |
| CE | Channel estimation |
| CDMA | Code division multiple access |
| CNN | Convolution neural networks |
| CP | Cyclic prefix |
| DL | Deep learning |
| DNN | Deep neural network |
| FC | Fully connected |
| FFT | Fast Fourier transform |
| FU | Far user |
| GRU | Gated recurrent units |
| ICI | Inter carrier interference |
| ISI | Inter symbol interference |
| IFFT | Inverse fast fourier transform |
| LS | Least squared error |
| LSTM | Long short-term memory |
| MIMO | Multiple-input, multiple-output |
| ML | Maximum likelihood |
| MMSE | Minimum mean squared error |
| MSE | Mean squared error |

# List of Abbreviations

| Abbreviation | Definition |
|---|---|
| NOMA | Non orthogonal multiple access |
| NU | Near user |
| OFDMA | Orthogonal frequency division multiple access |
| OMA | Orthogonal multiple access |
| QoS | Quality of service |
| QPSK | Quadrature phase shift keying |
| ReLU | Rectified linear unit |
| RNN | Recurrent neural networks |
| SC | Superposition coding |
| SER | Symbol error rate |
| SIC | Successive interference cancelation |
| SINR | signal-to-interference-noise ratio |
| SNR | Signal-to-noise ratio |
| TDMA | time Division multiple access |
| UE | User's equipment |
| 5G | fifth-generation |
| 1-d CNN | One-dimension convolution neural networks |

# List of Symbols

| Symbol | Definition |
|---|---|
| $b$ | **Correlational bias at (t)** |
| $\overline{C_t}$ | **Candidate Cell state** |
| $C_t$ | **Cell state** |
| $E$ | **Signal to noise ratio(S/N)** |
| f | **Transfer function** |
| $F$ | **Size of filter** |
| $f_t$ | **Forget gate at time step(t)** |
| G | **Cost function** |
| $h_t$ | **Current memory gate** |
| $\overline{h}_t$ | **Candidate memory gate** |
| $h_n(t)$ | **Impulse response from a multipath channel** |
| $\widehat{H}_{PLS}$ | **The estimate channel response** |
| $i_t$ | **Input gate at time step($t$)** |
| K | **The kernel size** |
| $l$ | **Number of paths** |
| $mp$ | **The number of pilots in one OFDM symbols** |
| $n$ | **Number of user** |
| N | **Total number of user** |
| $O_F$ | **The output feature map** |
| $o_t$ | **The gate output** |
| P | **Transmitted power** |
| $P_a$ | **The amount of padding** |
| R | **Data rate** |
| $\mathrm{R}_{\mathrm{H_P Y_P}}$ | **The cross covariance matrix between $\mathbf{H_P Y_P}$** |
| $\mathrm{R}^{-1}{}_{\mathrm{Y_P Y_P}}$ | **Inverse auto covariance matrix of $\mathbf{Y_P Y_P}$** |
| $r_t$ | **The reset gate** |
| S | **The stride** |
| $\tanh(x)$ | **Hyperbolic tangent activation function** |
| $W$ | **The weighting matrix** |

# List of Symbols

| Symbol | Definition |
|---|---|
| $w_n$ | **White Gaussian Noise** |
| $x(t)$ | **Current input** |
| $X_n$ | **Total transmitted signal for user n** |
| $x_p$ | **Diagonal matrix of pilots** |
| $Y$ | **Received signal** |
| $z_t$ | **The update gate** |
| $\alpha$ | **Total power allocation factor** |
| $\delta^2$ | **Noise variance** |
| $\rho_{n,l}$ | **The complicated channel gain** |
| $\tau_{n,l}$ | **The equivalent delay in time of the $l$ th component for user ($n$) with multiple paths** |
| $\sigma(\gamma)$ | **Sigmoid function** |
| $\sigma(x_c)$ | **Softmax function** |
| $\sigma$ | **Activation function** |

# Accepted for Publication

- M. N. Alderhomi , R. AL-Musawi and Hilal Abod Al-Libawy, “Deep Learning Based signal Detection in NOMA Systems:A Review,” *2th International Conference on Adances in Engineering Science and Technology (AEST-2022)*.

# Publication

- M. N. Alderhomi , R. AL-Musawi and Hilal Abod Al-Libawy, “Exploiting One- Dimensional Convolutional Neural Networks for Joint Channel Estimation and Signal Detection in Non- Orthogonal Multiple Access Systems,”*Journal of University of Babylon for Engineering Sciences*,vol.31,no.4,2023.

# Chapter One Introduction

# CHAPTER ONE
# INTRODUCTION

## 1.1 Overview

In response to escalating demands for rapid data transmission, minimal latency, and pervasive connectivity, there is an ever-growing necessity for more streamlined wireless communication systems. Non-Orthogonal Multiple Access (NOMA) technology has emerged as a promising antidote to enhance spectral efficiency significantly. This innovative paradigm facilitates the concurrent service of multiple users on identical frequencies, albeit with distinct power allocations. The outcome is a remarkable boost in spectrum utilization efficiency and transmission rates [1,2].

The fifth-generation (5G) wireless communication technology has a lot of potential with the NOMA approach[3].Incoming information is processed based on the channel condition between users and a base station or Quality of Service (QoS) requirements. Successive Interference Cancellation (SIC) helps decode these signals. Hybrid OFDM-NOMA systems leverage the strengths of NOMA and Orthogonal Frequency Division Multiplexing (OFDM) to efficiently allocate resources, enhance network capacity, and address the challenges posed by an increasing number of users in wireless networks [4].SIC heavily depends on accurate channel estimation and traditional methods such as Least Squares (LS), Minimum Mean Square Error (MMSE) and Maximum Likelihood (ML) are often employed for this purpose. LS is a simple and widely used channel estimation method that aims to minimize the sum of squared errors between the estimated and received signals. MMSE estimation takes into account both the desired signal and the interference, using statistical principles to estimate the channel. It can provide more accurate estimates compared to LS. ML estimation seeks to find the channel estimates that maximize the likelihood of the received signal given the channel model. It is considered optimal in terms of accuracy

but can be computationally intensive. Imperfect channel estimation can introduce errors in a hybrid OFDM-NOMA system that relies on (SIC) for signal detection [5].

To overcome the problem of imperfect SIC and its complexity, researchers have proposed using Deep Learning (DL) to detect hybrid OFDM-NOMA signals at the receiver side [6]. DL is a branch of machine learning that uses artificial neural networks to learn from data. In this situation of NOMA, DL algorithms can be trained to detect and decode signals by learning from a massive number of datasets NOMA signals. DL-based NOMA detection has been shown to overcome traditional channel estimation methods especially in cases where the channel conditions are hard to estimate precisely [7,8]. Recently, many studies have been conducted on DL-assisted NOMA signal detection and channel estimation to reduce Symble Error Rate (SER) where the results have been impressive [9].

## 1.2 Literature Review

This section presents a scientific review of current research on deep learning (DL) applications in (NOMA) system for signal detection and channel estimation. The review encompasses an overview of recent research on NOMA and its benefits for wireless communication systems. In addition, the literature review delves into recent advancements in DL-based signal detection and channel estimation in NOMA systems, comparing their performance with conventional methods. Several studies have used recurrent neural networks (RNN) for channel estimation and signal detection in NOMA system, while others have used convolutional neural networks (CNN) or hybrid models to achieve superior performance.

## A. Recurrent Neural Networks ( RNN)

**In 2019, J. Thompson et al.** [10] presented DL -long short term memory (LSTM) for the channel -estimation and signal- detection by jointly recovering transmitted signal for both users using a two-user hybrid OFDM-NOMA system. Their proposal has proven its superiority over traditional methods (SIC) receiver and compared to traditional channel estimate methods, it is more resistant to limited spectrum parameters like signal strength, pilot symbols, and cyclic prefix, but their proposal was suffering from overfitting because of the training accuracy more than testing accuracy. When a DL network overfits, it tries to transfer learning from the training sample to the test sample, which is separated from the training sample to assess the network's performance on data that it has never seen before.

**In 2022, A. Hilal et al.** [11] long short-term memory [LSTM] was suggested and the production of a testing set at different signal-to-noise ratios (S/N) by changing the number of [LSTM] layers, The result shows their approach has better performance over the recent DL model and traditional methods such as LS, MMSE and ML system in term SER and reduce the overfitting that appears in Previous approaches. However, the results of their proposed approach outperform traditional methods such as (ML) by about 2db and LSTM in 2019, J. Thompson by about 3db.

**In 2022, S. Pandya et al.** [12] presented DL-LSTM to simultaneously identify signals and estimate channel parameters. They use the same scenario as recent studies but modify some training option parameters, such as learning rate (0.03) and batch size (25000). Although the DNN outperforms as the number of batches increase, convergence is slowed since more updates are required. However, compared to other established techniques that have been applied in this field, their proposed model is better in term of SER but need a long time to train. However, the results of their proposed approach outperform traditional

methods such as (ML) by about 1.5db when reducing cyclic prefix (CP) and it is identical to ML when reducing the number of pilots.

**In 2022, D.V. Rahman et al.** [13] presented another type of RNN bidirectional-LSTM [BILSTM] where the received signal feed into end to-end BILSTM layer, a development of the unidirectional LSTM is the bidirectional LSTM. Right to left and left to right are the two directions that Bi-LSTM aims to collect information from. Their proposal beat other DL models (CNN, LSTM) and the traditional method for signal detection at (SIC) receiver in terms of sample error rate. However, the results of their proposed approach outperform traditional methods such as (ML) by about 0.8db and other DL models (CNN) by 3db.

**In 2022, A. Bhatt et al.** [14] presented Non-Orthogonal Multiple Access (NOMA) depends on DL- RNN to detect signals and make channel estimations from one operation. Where they used the long short-term memory approach (LSTM) at a frequency-flat Rayleigh distributed fading channel. They utilized a 72-subcarrier OFDM framework with packet data. The total number of hidden layers used in DL-LSTM is 128. When the normal situation of the system their approach was better than LS but worse than that of MMSE in term SER. They reduced some of the parameters that affect the system, such as (CP) where their proposal proved superior to traditional methods such as (MMSE and LS). Also, test their approach at different learning rates, their results were acceptable. They calculated the time required for training and found that there was no effect on time when increasing the number of paths. However, the results of their proposed approach outperform traditional methods such as (MMSE and LS) by about 1.9db when reducing the number of pilots.

## B. Deep Neural Networks (DNN)

**In 2020, M. A. Aref et al.** [15] deep neural networks (DNN) was suggested to aid signal detection and channel estimation at the receiver side

in the uplink MIMO-NOMA system. They suggested using a single DNN to decode the signal for each user at every SIC stride. Their approach reduced error propagation and system complexity where need fewer K-1 DNNs than DL-SIC. It can be seen from their research that if anything goes wrong with the decoding of the user signals, an error will occur on the receiver end because the decoding of the second user is based on the decoding of the first user, the third user depends on the first and second users. Also, they did not compare their findings to the traditional methods such as (ML, MMSE, and LS), which is more comparable to the ideal system and is used as a baseline in most studies. However, the results of their proposed approach outperform the other DL- SIC by about 2db.

**In 2021, A. L. Ha et al.** [16] presented deep neural networks with two architectures of DNN_1 and DNN_2 was suggested to aid channel estimation in the MIMO-OFDM framework utilizing the two various fading multi-path channel model situations depending on the TDL _ A system established in the 5G technology. The suggested DNN structure contains three hidden layers which include a large number of neurons with an input layer and an output layer. Using the channel estimates from the LS prediction as an input, the DNN learned the current channel information. However, the results of their proposed approach outperform the traditional methods such as (LS and LMMSE) in terms of mean squared error (MSE) by about 5 db.

## C. Convolution Neural Networks (CNN)

**In 2020, S. Isaac et al.** [17] the convolutional neural network (CNN)-based SIC scheme was suggested to enhance the efficiency of the single base station and several user NOMA systems. On the other hand with current SIC methods, the suggested CNN-based SIC method can successfully reduce the

error caused by a lack of SIC. Their proposed architecture consists of two convolutional layers, followed by a max pooling layer. A pair of dense layers with 256 and 128 neurons was then combined after two convolution and pooling layers. Every CNN layer's output is determined by its activation function, in this study they used sigmoid and exponential linear unit (ELU) as activation functions. However, the simulation results show that the CNN-based SIC method can effectively mitigate the problem of traditional SIC and achieve good detection accuracy.

**In 2021, Y. Xie et al.** [18] provide a hybrid CNN feature extractor and time-series LSTM layer to meet the NOMA-OFDM challenge. They suggested dividing the data of the received signals using a CNN-based feature extraction, to meet inter-carrier and inter-symbol interference. The LSTM layers are suggested to solve the significant ISI caused by the multi-path channel effect, and the CNN-based feature extractor simulates the conventional process to deal with ICI caused by a doppler shift. Their method operates in 5G situations at a doubly-selective tapped-delay line channel. It has been demonstrated that the proposed DL reduces the error rate when there are not enough pilots, and improves SER efficiency by about 4db in comparison using the conventional MMSE-SIC approach. They used an end-to-end framework, combining channel estimation and signal detection. When compared to the MMSE-SIC technique, the proposed DL has a less complicated computation since the MMSE-SIC needs the matrix inversion algorithm.

**In 2022, D. Kanzariya et al.** [19] Multiple convolutional layers and numerous hidden layers are utilized in an efficient deep neural network for 5G communication. To reduce signal error rates and instantly identify the channel characteristics of MIMO-NOMA, the NOMA-MIMO-DL architecture solves the data detection challenge. They were used (2×2, 4×4 and 8×8) MIMO-NOMA system with two users one has good condition channel and the other has

bad condition channel. Their suggestion outperforms the other DNNs used for MIMO-NOMA signals detection in terms of SER, where the performance of their approach enhancement when the signal-to-noise ratio increases and goes under $10^{-6}$at 25 db. However, the results of their proposed approach outperform the other DL MIMO-NOMA by about 5db.

**In 2022, R.S.H. AL-Musawi et al.** [20] provide Convolutional neural network (CNN)-based deep learning (DL) network, in which data frames are converted into 2-D images and fed into a three-layer CNN for labeling in a single process. Over an adjustable filter was learned from input samples, CNN works as a feature extractor. They used a two-user device, a 64-subcarrier OFDM system, and 1000 packets to demonstrate the effectiveness of their approach. With two-user, the CNN-depend DL automatically handles channel estimation and decoding. Approximately 80% precision was attained during the training and testing process. However, the results of their proposed approach outperform traditional methods such as (ML) even at a low signal to noise ratio and reduced cyclic prefix by about 8db.

**In 2022, A. H.Ali et al.** [21] presented a one-operation deep learning model containing LSTM and convolution neural network (CNN) Portion, where their investigation shows a change incoming OFDM-NOMA packets into a two dimension image and transfers this image for the CNN portion that has increased efficiency and decreased overfitting with LSTM methods in the previous studies. However, the results of their proposed approach outperform traditional methods such as ML even at a low signal to noise ratio and reduced cyclic prefix by about 1.5db and the other DL methods such as enhancement LSTM by about 6.5db.

**Table (1.1): Summary of literature review**

| References | DL-type | Transmission scenario | Users number | No. of antennas | Performance in term SNR |
|---|---|---|---|---|---|
| J. Thompson et al [10]. | LSTM 128 layer | Uplink | Two user | Single | Outperform LS,MMSE and ML. |
| A. Hilal et al [11]. | LSTM 64 layer | Uplink | Two user | Single | Outperform MLby 2db and outperform LSTM in [10] by 3db and reduced overfitting. |
| S. Pandya et al [12]. | LSTM | Uplink | Two user | Single | Outperform ML by 1.5db when reduce CP and identical to ML when reduce P |
| D.V.Rahman et al [13]. | BILSTM | Uplink | Two user | Single | Outperform ML by 0.8 and outperform other DL models (CNN) by 3db |
| A.Bhatt et al [14]. | LSTM 128 layer | Uplink | Two user | Single | Outperform (MMSE , LS) by about 1.9db |
| M. A. Aref et al [15]. | DNN | Uplink | Four user | Single | Outperform the others DL-SIC by 2db |

| | | | | | |
|---|---|---|---|---|---|
| A.L. Ha et al [16]. | DNN | Down link | Two user | double | Outperform (LS,LMMS) by 5db |
| S. Isaac et al [17]. | CNN | Down link | Two user | Single | Outperform the other DL methods |
| Y. Xie et al [18]. | CNN + LSTM | Uplink | Two user | Single | Outperform (MMSE) by 4db |
| D.Kanzariya et al [19]. | CNN | Down link | Two user | Single MIMO channel | outperform the other DL MIMO-NOMA by about 5db |
| R.S. ALMusawi et al [20]. | CNN | Uplink | Two user | Single | Outperform ML by 8db |
| A. H. Ali et al [21]. | CNN + LSTM | Uplink | Two user | Single | Outperform ML by 1.5db and Outperform enhancement LSTM in [11] by 6.5db |

## 1.3 Problem Statement

In light of the aforementioned survey, the efficacy of NOMA is intricately tied to the precision of channel estimation and the intricacy of SIC at the receiver. While pilot-based techniques and the advent of DL have demonstrated potential in mitigating these hurdles, there remains an opportunity for further enhancements in terms of accuracy, complexity, and scalability.

## 1.4 Thesis Objectives

1. To design and develop an end-to-end deep learning-based NOMA system for uplink scenarios.
2. To compare the performance of the proposed end-to-end deep learning-based NOMA system with the existing pilot-based channel estimation techniques in terms of SER performance , complexity, and computational efficiency .
3. To investigate the impact of varying channel conditions, such as fading, cyclic prefix, and pilot, on the performance of the end-to-end deep learning-based NOMA system.
4. Calculating the training time for the proposed deep learning methods and comparing them with other deep learning systems that are used in this field.
5. To propose any necessary modifications or enhancements to the end-to-end DL-based OFDM-NOMA system to further improve its performance and scalability.

## 1.5 Thesis Layout

In addition to chapter one, this thesis is divided into different chapters to present the proposed models for signal detection and channel estimation in NOMA-OFDM systems. Chapter two gives an overview of multiple access methods and explains the key concepts of NOMA, its benefits, and how it compares to OMA. The chapter also covers the basics of NOMA characteristics in both downlink and uplink scenarios, pilot-based channel estimation, and the types of deep learning algorithms used in this thesis. Chapter three focuses on the proposed models and explains each component of the models in detail. Chapter four presents the simulation results and discusses how well the proposed models performed. Finally, chapter five concludes the thesis by summarizing the

contributions of this work and suggesting future research directions to improve signal detection and channel estimation.

# Chapter Two

# Theoretical Background

# Chapter Two

## Theoretical Background

### **2.1** Introduction

As the demand for high-capacity and reliable communication services increases, the limitations of Orthogonal Multiple Access (OMA) techniques such as Frequency Division Multiple Access (FDMA), Time Division Multiple Access (TDMA), Code Division Multiple Access (CDMA), and Orthogonal Frequency Division Multiple Access (OFDMA) become apparent. These limitations include lower spectral efficiency and higher complexity, making them less suitable for next-generation wireless networks [22].

Non-Orthogonal Multiple Access (NOMA) has emerged as a promising alternative to OMA techniques due to its ability to support a large number of users simultaneously and efficiently use available spectrum resources. NOMA utilizes power domain multiplexing to allow multiple users to share the same frequency resource, which leads to higher spectral efficiency and more effective use of network resources. In contrast, OMA techniques allocate orthogonal resources to each user, leading to less efficient use of the available spectrum and potentially lower user capacity. Moreover, NOMA has been shown to have superior performance in challenging scenarios such as weak signal conditions and high mobility environments. NOMA also enables more effective energy consumption by mobile devices, allowing for longer battery life and reducing overall energy consumption in the network [23]. In conclusion, NOMA offers several advantages over OMA techniques, including higher spectral efficiency, increased capacity, and improved energy efficiency. These benefits make NOMA a promising candidate for next-generation wireless networks and an important consideration for network designers and operators [24].

Superposition coding is a key concept in Non-Orthogonal Multiple Access (NOMA), where multiple users' data is superimposed on a single channel using different power levels [25]. The receiver uses successive interference cancellation (SIC) to decode the signals of each user by iteratively removing the decoded signals of previously decoded users. However, as the number of users increases, SIC becomes increasingly difficult to decode and separate user signals [26,27].

One solution to this challenge is the use of deep learning techniques, such as end-to-end deep learning models. These models can perform joint channel estimation and signal detection in NOMA systems, thereby eliminating the need for perfect channel estimation required in SIC-based strategies [28]. End-to-end deep learning models have been shown to be effective in improving the performance of NOMA systems in several ways. For instance, they can significantly reduce the computational complexity required for signal detection and channel estimation, making it more efficient than SIC-based strategies. Additionally, these models can learn the channel characteristics and optimize the detection parameters for different channel conditions and user scenarios.

## 2.2 Orthogonal Multiple Access (OMA) Techniques

Orthogonal Multiple Access (OMA) is a popular technique used in wireless communication systems for resource allocation to multiple users. The basic idea of OMA is to allocate orthogonal resources, such as time slots, frequency bands, or codes, to different users to avoid interference between them. The typical OMA technique is illustrated in Figure (2-1).

Some popular OMA techniques used in mobile networks include Frequency Division Multiple Access (FDMA), Time Division Multiple Access (TDMA), Code Division Multiple Access (CDMA), and Orthogonal Frequency Division Multiple Access (OFDMA).

FDMA is used in 1G mobile networks and divides the frequency band into multiple sub-channels, with each user assigned a dedicated sub-channel for communication.

TDMA is used in 2G mobile networks and allocates time slots to different users, allowing multiple users to share the same frequency band.

CDMA is used in 3G mobile networks and assigns a unique code to each user to differentiate between them.

OFDMA is a popular OMA technique used in 4G and 5G mobile networks. It divides the frequency band into orthogonal sub-carriers and allocates them to different users. OFDMA can provide a high degree of flexibility in resource allocation, allowing for efficient use of the frequency band and support for high data rates [29].

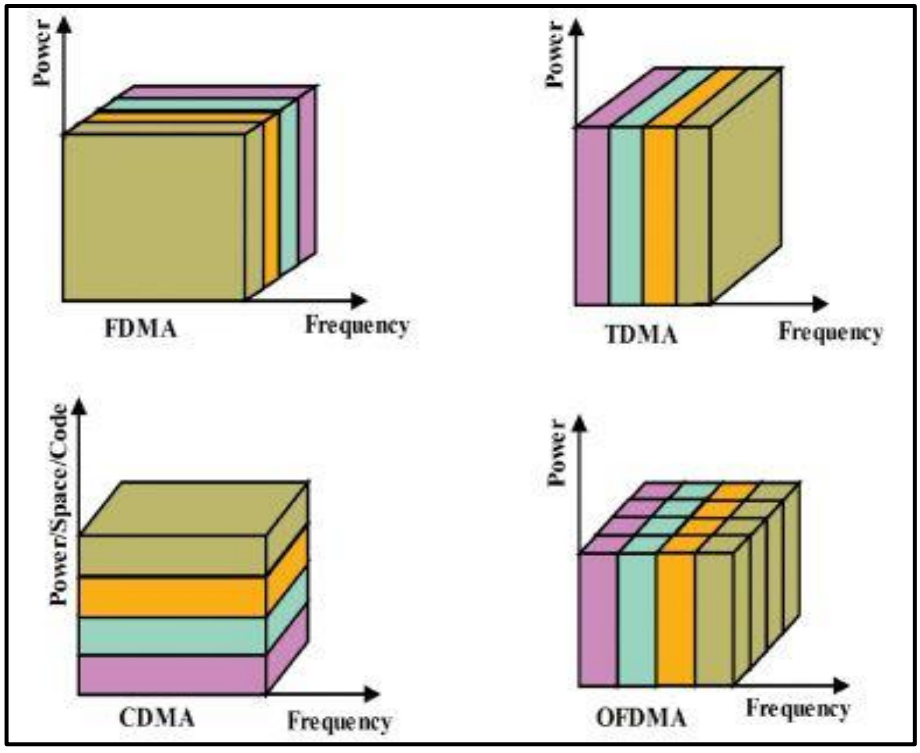


Figure 2-1 Orthogonal multiple access (OMA) [30].

## 2.3 Non-Orthogonal Multi Access System ( NOMA)

The increasing demands of future communication networks have created a need for technologies that can meet the requirements for high bandwidth efficiency, low latency, and user fairness. However, OMA has not been able to satisfy these demands [31,32]. To meet these additional expectations, a modern approach called NOMA has been proposed [33]. The NOMA approach can be used in the construction of the fifth generation (5G) of wireless networks in the field of wireless communication systems [34].

Figure (2-2) provides a visualization of the differences in power allocation between OMA and NOMA approaches. NOMA achieves its high efficiency by using a superposition coding (SC) method on the transmitter side and the (SIC) algorithm on the receiver side [35]. This combination of techniques can increase the capacity of the bandwidth used by NOMA, which makes it a promising candidate for meeting the demands of modern communication systems.

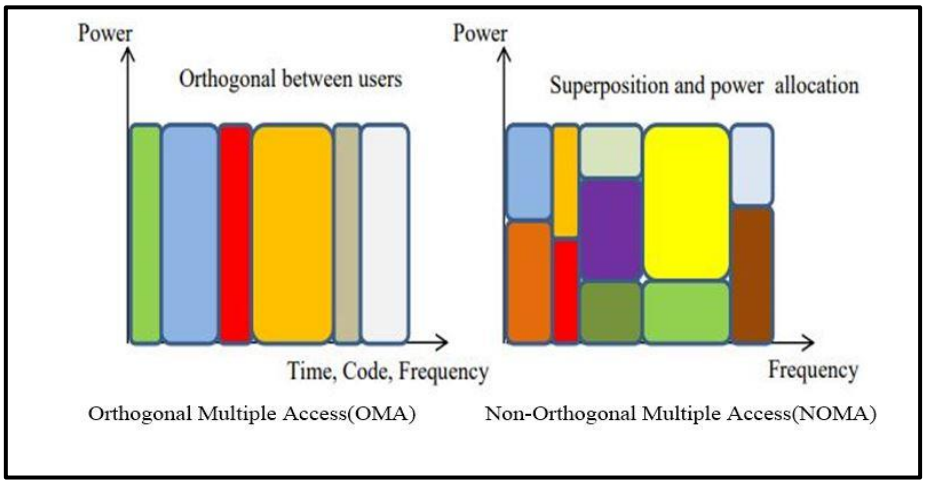


Figure 2-2 Power distribution in multiple-user access systems [32].

To enable NOMA on the transmitting end, the use of superposition coding, also called power domain multiplexer, is necessary. When two users are present, their signals (x1 and x2) are first multiplied by different power allocation factors based on the channel condition. These signals are then combined

through superposition, where the signals from both users are added together as total transmitted signal $\left(X_{super.p}\right)$ [32].

$$X_{super.p} = \sqrt{\alpha_1}\, x_1 + \sqrt{\alpha_2}\, x_2 \quad (2.1)$$

Where $\alpha_1$ , $\alpha_2$ are power allocation factors for signal1and signal 2 respectively.

$$\alpha = \alpha_1 + \alpha_2 = 1 \quad (2.2)$$

Where $\alpha$ total power allocation factor.

The power allocation is determined based on the user's distance from the base station. For users located far from the base station with a low channel condition, a higher power allocation is given. Conversely, users located near the base station with a high channel condition receive a lower power allocation. The far user has low channel condition and high power allocated, while the near user has high channel condition and low power allocated.

To decode the signals in NOMA, the successive interference cancellation (SIC) algorithm is used, which is an iterative process that decodes signals in order of decreasing power level. The signal with the highest power is decoded first, followed by the data of the user with the second-highest power. This process is repeated until all user information is decoded. The resulting signal received by the base station (BS) after decoding the compact signal from $n$ users is given by Eq. (2.3) [35].

$$\mathrm{Y}_{NOMA} = \sum_{n=1}^{N} \sqrt{\alpha_n}\, x_n \quad (2.3)$$

The signal Y is subjected to direct decoding to extract the high-power signal( $x_1$), associated with the distant user. Concurrently, the signal ( $x_2$), which possesses a lower power allocation, is considered as interference and is effectively treated as noise during this process. Following the successful

decoding of the high-power signal, ( $x_1$), it is multiplied by its corresponding power allocation factor. Subsequently, the result is subtracted from the total received signal, Y, to further isolate and process the remaining signals.E.q (2.4) present this [35].

$$Y_{NOMA} - \sqrt{\alpha_1}\, x_1 = \sqrt{\alpha_2}\, x_2 \quad (2.4)$$

Lastly, the signal resulting from the preceding step (as described in E.q.2.4) is subject to decoding. The outcome of this decoding operation yields the signal corresponding to the near user, represented as ($x_2$). Figure (2-3) illustrates the SIC NOMA algorithm, portraying the sequential signal processing steps.

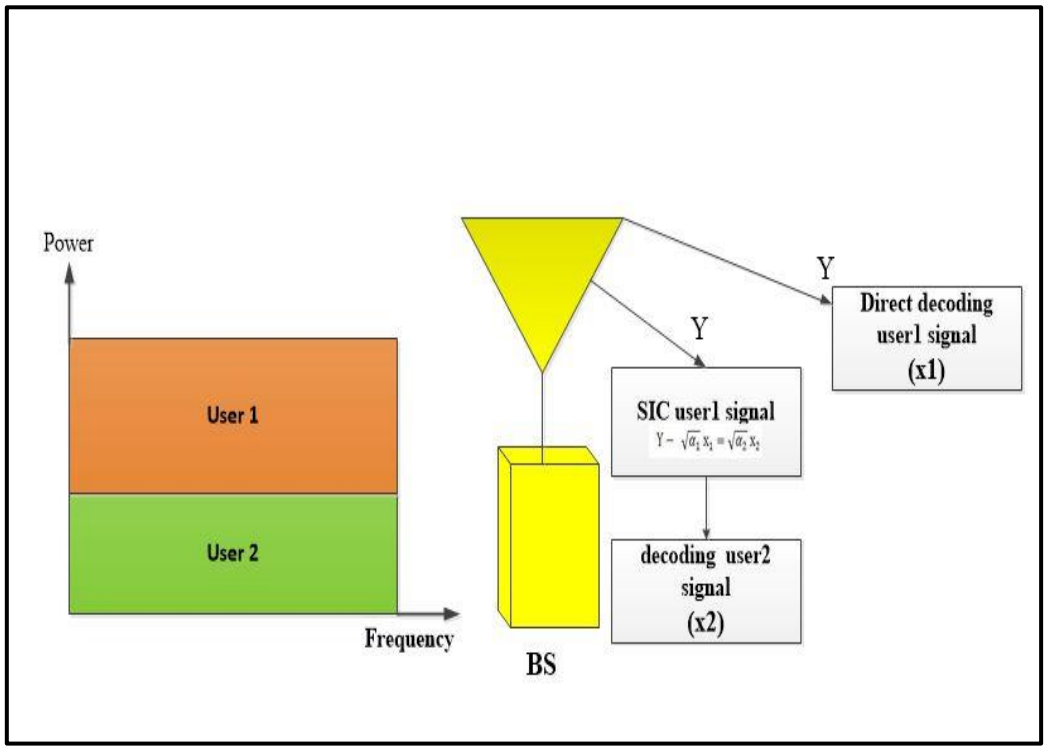


Figure 2-3 SIC NOMA algorithms [35].

## 2.4 NOMA's Benefit

Several research studies have compared the performance of NOMA and OMA in different scenarios, and have shown that NOMA can outperform OMA in terms of bandwidth efficiency. For example, some studies have shown that

NOMA can achieve up to 35% higher downlink spectral efficiency and up to 95% higher uplink bandwidth efficiency compared to OMA[32]. However, the actual performance of NOMA and OMA depends on the specific system parameters and deployment scenarios. NOMA has several characteristics and features that make it possible for it to satisfy the requirements of the coming generations of wireless communication technologies and beyond while also resolving the challenges that OMA suffered. Here are some of the characteristics which permit NOMA from beating OMA.

### 2.4.1 The Bandwidth Performance.

The Orthogonal Frequency Division Multiple Access (OFDMA) and other Orthogonal Multiple Access (OMA) techniques suffer from low rate efficiency because they allocate a certain frequency bandwidth to each user's equipment (UE) regardless of the UE's channel conditions. This is because OFDMA and OMA techniques use orthogonal subcarriers to separate the transmissions of different UEs, which means that the same subcarrier cannot be used simultaneously by multiple UEs. This results in a fixed allocation of frequency bandwidth for each UE, regardless of their channel conditions. In contrast, NOMA allowed for multi-users to utilize one frequency bandwidth but with a distinct power allocation factor [36]. A **Far** user will utilize the same frequency source as a **near** user, and SIC procedures could recognize interference in both users' receivers. As a result, the potential of attaining better bandwidth efficiency as illustrated in Figure (2-4).

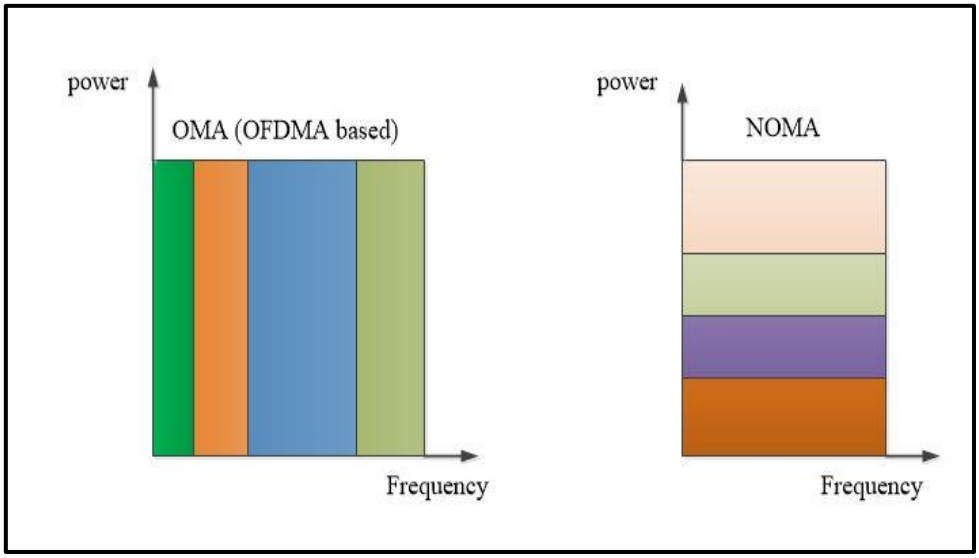


Figure 2-4 Bandwidth efficiency differences between OMA and NOMA [36].

### 2.4.3 NOMA with Fairness To Far/Weak User

OFDMA suffers from fairness issues in situations where there are users with different channel conditions. This is because OFDMA allocates the same amount of resources to all users, regardless of their channel conditions. Users with better channel conditions can use these resources more efficiently, while users with poorer channel conditions may experience lower throughput or even packet loss [37]. On the other hand, Non-Orthogonal Multiple-User Access (NOMA) provides service to multiple users concurrently, which promotes user equity and enhances system throughput [38].

### 2.4.3 Suitability

(NOMA) has been studied and considered as part of various communication standards, including the 3rd Generation Partnership Project (3GPP) standards, which govern cellular communication technologies. NOMA's principles can be integrated into future communication frameworks with relatively fewer structural changes than may be required for other technologies. [39].

### 2.4.4 Transmission Time Delay and The Signal with Low Cost

OMA utilizes access permissions to facilitate communication between users and the BS [40]. To start a communication, the user equipment should transmit a schedule demand to the BS. After scheduling the uplink transmission after receiving the demand, the BS informs the user that the connection is clear by sending a clear message. As just a result, transmission latency and signaling cost all significantly increase. Before data transfer, long-term evolution (LTE) wireless access needs about 15.4 ms making it challenging for 5G networks to achieve ultra-low latency requirements (e.g., less than 1ms). The transmitter utilizes multiple access for NOMA uplink communication without making access requests. While NOMA offers lower transmission latency, using successive interference cancellation (SIC) with a massive number of users can introduce long delays in the detection process. [41].

### 2.4.5 The Data rate

In comparison to current orthogonal multiple access (OMA) systems like time-division, multiple access (TDMA), and frequency-division multiple access (FDMA), non-orthogonal multiple access, or NOMA, is a potential multiple access method for 5G and beyond. This is so that numerous users can send data simultaneously on the same frequency channel as a result of NOMA's ability to provide the same time-frequency source in a non-orthogonal pattern. Therefore, the communication system can operate at a higher achievable rate and with greater capacity. In a downlink communication system with a base station (BS) and N users' equipment, assuming a channel $h_n$ between the BS and the N user, we have: far user (FU) has a low channel condition $h_1$ and a near user (NU) has a high channel condition $h_2$.Where $h_1 < h_2 < \cdots h_N$ .

If we take the NOMA scenario then the total transmitted data for the two users can be presented in Eq.(2.5)

$$X_{NOMA} = \sqrt{p}\ \sum_n^N \sqrt{\alpha_n}\ x_n \quad (2.5)$$

Where $p$ represent total transmitted power for two users. The total received signal at user $n$ is given by Eq.(2.6)

$$Yn_{NOMA} = X_{NOMA} * h_n + w_n \quad (2.6)$$

Where $h_n$ , $w_n$ channel condition and AWGN with zero mean and variance = $\sigma^2$ at user $n$ respectively.

Then the achieve rate at any user $n$ can be written as Eq.( 2.7)

$$\boldsymbol{Rn}_{(\boldsymbol{NOMA})} = \log_2(1 + Yn_{NOMA}) \quad (2.7)$$

In other hand the total transmitted data for the two users OMA system can be presented in Eq.(2.8)

$$X_{OMA} = \sqrt{p}\ (x_1 + x_2) \quad (2.8)$$

The total received signal at user $n$ is given by Eq.(2.9)

$$Yn_{OMA} = X_{OMA} * h_n + w_n \quad (2.9)$$

Then the achieve rate at any user $n$ can be written as Eq. (2.10)

$$\boldsymbol{Rn}_{(\boldsymbol{OMA})} = \frac{1}{N}\log_2(1 + Yn_{OMA}) \quad (2.10)$$

From this, we conclude that the achievable rate from NOMA doubles in comparison to OMA [42].Figure (2-5) presented OMA,NOMA rates at different Signal to Noise Ratio(SNR).

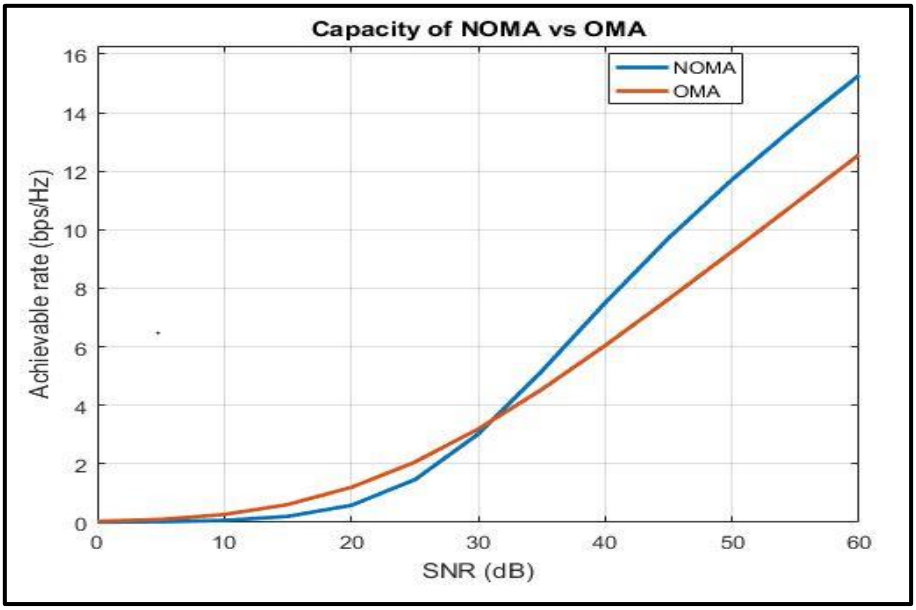


Figure 2-5 Comparison between NOMA and OMA in term rate capacity [42].

**Table 2-1 Comparison between NOMA and OMA**

| | Advantages | Disadvantages |
|---|---|---|
| **OMA** | • Receiver sophistication is low. | • Its bandwidth efficiency is poorer.<br>• It is servicing a specific number of users.<br>• Less rate from NOMA<br>• High delay time (latency)<br>• Absence of user fairness |
| **NOMA** | • Its bandwidth efficiency is higher.<br>• It is servicing a high number of users.<br>• High data rate<br>• User fairness appears in NOMA<br>• higher service quality<br>• NOMA is cooperative | • Receiver side complexity is high.<br>• Since the near user depend on far user signal, imperfect SIC causes the system not to be reliable.<br>• Need high channel estimation |

## 2.5 Basic NOMA in Downlink and Uplink Characteristics

Non-Orthogonal Multiple Access (NOMA) can be applied in both the downlink and uplink of wireless communication systems. In the downlink scenario, the base station (BS) or access point serves as the transmitter, and multiple users or devices are the receivers. In the uplink scenario, the users or devices themselves serve as transmitters, and the base station or access point is the receiver. Uplink allows multiple users to transmit their data to the BS simultaneously on the same frequency resources.

### 2.5.1 NOMA Downlink

NOMA permits a base station to send several signals in the downlink direction to various users while utilizing the same time-frequency resource. Using successive interference cancellation (SIC) methods, NOMA downlink enables users to decode their original transmission by superimposing several signals of varying power values. Figure (2-6) show NOMA downlink system. In general, the base station sends a collection of $(\boldsymbol{x})$ signals to $n$ user $(n = 1,2,3,\dots.N)$ it is denoted as $x_n$ and transmitting power $p_n$ . Collecting of $p_n$ $(n = 1,2,3,\dots.N)$ is equal total transmitted power. The equation below can be used to represent the transmitted signal.

$$x = \sum_1^n \sqrt{p_n}\ x_n \tag{2.11}$$

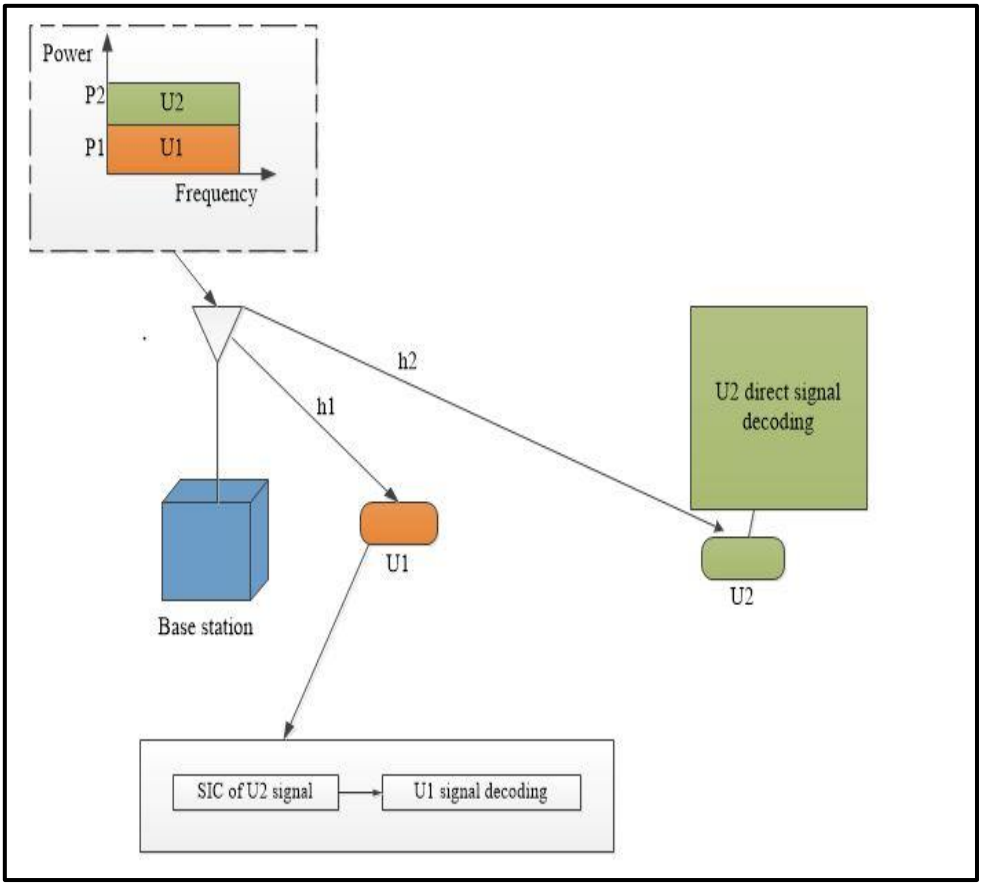


Figure 2-6 NOMA downlink system with single base station and two users [43].

The signal that the user ($n$ ) received thus can be represented by Eq.(2.12)

$$y_n = h_n x + w_n \tag{2.12}$$

Where $h_n$ is represented complex channel coefficient between (BS) and the user $n$, $w_n$ is represented white Gaussian noise that is added at the (UE) $n$ including variance of noise ${\sigma_n}^2$ . At the user equipment end, the SIC approach is used to reduce the impact of the unwanted received signal parts. SIC is working according the location of user $n$ from base station and this depend on the channel's quality $\frac{|h_n|^2}{{\sigma_n}^2}$ this structure permits each user to successfully discover their signal and avoids signal interruption from other users [44]. To improve their received signal-to-interference-noise ratio (SINR) and ensure accurate detection, users with low quality channels should commonly obtain

greater power amounts. Users with better channel quality utilize the opposite technique. Despite near user having a low power level, there has a good probability that it will be able to identify its data. As a result, its receivers can apply the SIC approach [45].

The assumption: $\frac{|h_1|^2}{{\sigma_1}^2} > \frac{|h_2|^2}{{\sigma_2}^2} > \cdots > \frac{|h_n|^2}{{\sigma_n}^2}$ (2.13)

Users' power allocations can be distributed as follows:

$$p_{1n} < p_{n2} \ldots . < p_n \quad (2.14)$$

According to Figure (2-7), how user 1's throughput $R_1$ can be expressed:

$$R_1 = \log_2\left(1 + \frac{P_{1|h_1|^2}}{{\sigma_1}^2}\right) \quad (2.15)$$

Also the throughput for user2 $R_2$ can be expressed:

$$R_2 = \log_2\left(1 + \frac{P_{2|h_2|^2}}{P_{1|h_1|^2 + {\sigma_2}^2}}\right) \quad (2.16)$$

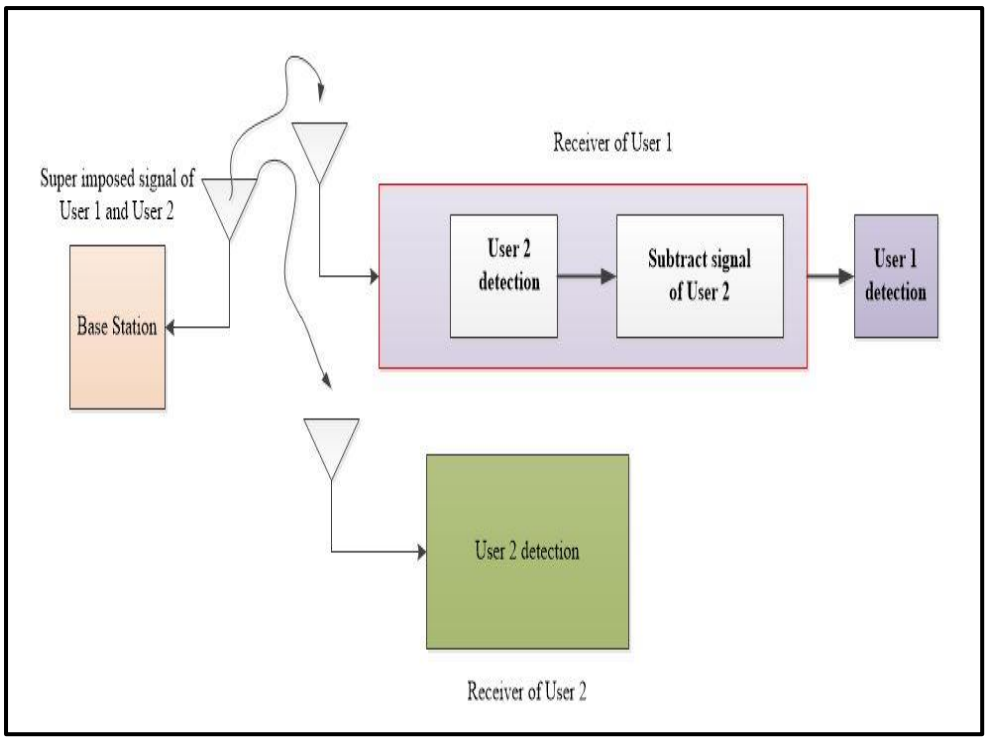


Figure 2-7 SIC decoding method at the user's end [46].

### 2.5.2 NOMA Uplink

The uplink NOMA system approximately resembles the downlink NOMA only there are minor differences in the precedence of signals detection at the base station. In the uplink NOMA, as shown in Figure (2-8), each user transmits its distinct signal $x_n$ to (BS) utilizing frequency band common from several UE[46]. In this instance, the transmitted and received data could be characterized as listed below:

$$X_n = \sum_1^n \sqrt{p_n}\ x_n \qquad n = 1,2,3 \dots, N \tag{2.17}$$

$$y_n = \sum_1^n X_n\, h_n + w_n \qquad n = 1,2,3 \dots, N \tag{2.18}$$

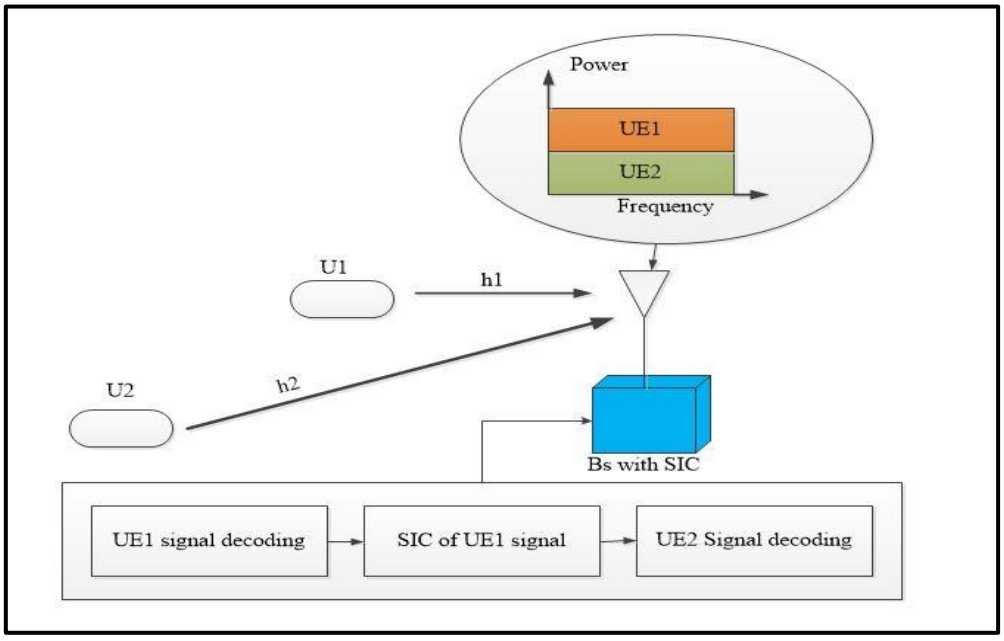


Figure 2-8 Uplink NOMA model with distributed power [46].

The signals in the uplink NOMA model may be detected in two scenarios: first, the base station detects the signal of the first user $x1$ which has a high conditional channel with small interference from the second user and can be neglected. Second, the base station subtracts the detected signal of user1 $(x1)$

from the total receive signal ($y$) at the receiver end and then decodes the residual signal as $x2$. Figure (2-9) shows this process.

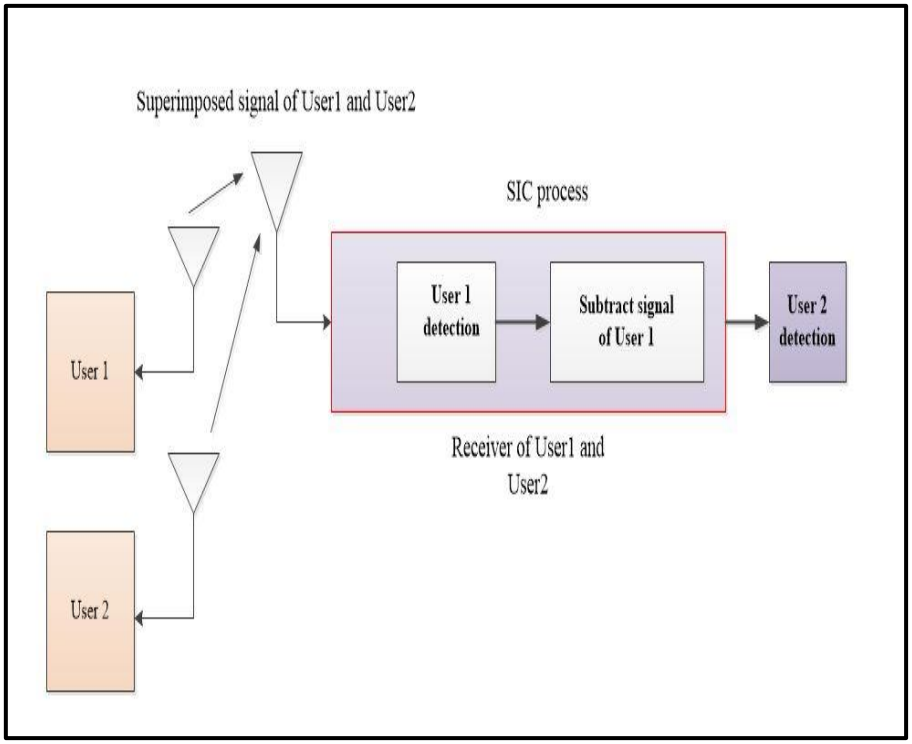


Figure 2-9 The SIC algorithms at uplink system [46].

Finally, the data rate or throughput of user 1 and user 2 is as follows:

$$R_1 = \log_2\left(1 + \frac{P_{1|h_1|^2}}{P_{2|h_2|^2+\sigma_1{}^2}}\right) \tag{2.19}$$

$$R_2 = \log_2\left(1 + \frac{P_{2|h_2|^2}}{\sigma_2{}^2}\right) \tag{2.20}$$

### 2.5.3 Uplink OFDM-NOMA System

Uplink OFDM-NOMA is a promising technology for future wireless communication systems, as it can accommodate multiple users more efficiently in scenarios with limited resources. However, it also requires sophisticated signal processing techniques at the receiver to decode the overlapping signals

from different users. In OFDM-NOMA multiple users are allocated the same set of subcarriers in the frequency domain. Each user's data is modulated and assigned a specific power level to create a superposition of signals. OFDM-NOMA can provide significant gains in spectral efficiency and overall system capacity compared to traditional orthogonal multiple access techniques, especially in scenarios with varying channel conditions among users[47].

## 2.6 Pilot-Based Channel Estimation

Accurate channel estimation is a crucial aspect of SIC-based NOMA systems. This is because any errors in the estimation of the channel can lead to interference leakage and reduced system performance [48]. In SIC-based NOMA, the decoding of signals from different users relies on accurate channel estimation, which is essential for the system's proper operation.

One effective approach to channel estimation is pilot-based techniques. Pilot-based techniques involve the transmission of known symbols (pilots) through the channel [49]. The received pilots are then used to estimate the channel parameters. LS (Least Squares), MMSE (Minimum Mean Square Error), and MLSE (Maximum Likelihood Sequence Estimation) are common pilot-based techniques used for channel estimation in SIC-based NOMA systems.

**LS** is a simple and computationally efficient pilot-based technique. It is based on the minimization of the mean square error between the estimated channel and the true channel. However, LS does not account for noise in the channel, which can result in inaccurate channel estimation[49].

**MMSE** is an improvement over LS as it accounts for noise in the channel. MMSE uses the a priori knowledge of the channel and the noise to minimize the mean square error between the estimated channel and the true channel. This results in better channel estimation performance than LS[50].

**MLSE** is the most accurate pilot-based technique as it uses a maximum likelihood criterion to estimate the channel parameters. MLSE finds the channel parameters that maximize the likelihood function given the received signal. However, MLSE is computationally complex and requires a large amount of processing power, making it unsuitable for real-time applications.

### 2.6.1 Least Squares (LS)

The Least Squares (LS) channel estimation technique is a method to estimate the channel coefficients of a communication system by minimizing the mean squared error (MSE) between the received signal and the estimated signal [50]. The goal is to find the channel coefficients that produce the smallest possible difference between the received signal and the estimated signal. The LS method seeks to find the value of X that minimizes the cost function G, which is given by:

$$G = \|H.X - Y\|^2 \quad (2.21)$$

Where H is the channel matrix, X is the estimate of the channel coefficients, Y is the received signal, and ||.||^2 denotes the squared Euclidean norm.

The LS solution can be obtained by setting the derivative of G with respect to X to zero, and solving for X:

$$\frac{dG}{dX} = 2 \cdot H^T \cdot (H.X - Y) \quad (2.22)$$

Solving for X, we get:

$$X = (H^T.H)^{-1} \cdot (H^T \cdot Y) \quad (2.23)$$

The LS solution provides an estimate of the channel coefficients that minimizes the MSE between the received signal and the estimated signal. However, the LS method can be sensitive to noise and may not work well in situations where the channel is rapidly changing.

### 2.6.2 Minimum Mean Square Error (MMSE)

MMSE better performance than LS but it is significant computational difficulty, specifically the requirement to perform matrix inversions whenever the information changes. If there is no correlation between the channel and the AWGN, the MMSE estimate of channel matrix *H* is given as [51]:

$$\widehat{\mathrm{H}}_{\mathrm{MMSE}} = \mathrm{R}_{\mathrm{H_P Y_P}} \mathrm{R^{-1}}_{\mathrm{Y_P Y_P}} \mathrm{Y_P} \quad (2.24)$$

Where $\mathrm{R}_{\mathrm{H_P Y_P}}$, $\mathrm{R^{-1}}_{\mathrm{Y_P Y_P}}$ and $Y_P$ : The cross covariance matrix between $\mathrm{H_P Y_P}$ ,inverse auto covariance matrix of $\mathrm{Y_P Y_P}$ and the matrix of received pilot signals at the receiver respectively.

### 2.6.3 Maximum likelihood Sequence Estimation (MLSE)

Maximal Likelihood Sequence Estimation is the best equalization method, it uses an estimation method rather than an equalizing filter, and it eliminates the problem of noise boosting [52]. The complexity of this method increases exponentially with the length of the time spread, making it useless on the majority of interesting channels. However, MLSE is more complex than LS and MMSE and needs a special algorithm such as Viterbi for signal detection. It requires complete information about the channel to work properly.

**In conclusion**, accurate channel estimation is crucial for SIC-based NOMA systems, and pilot-based techniques such as LS, MMSE, and MLSE are effective methods for channel estimation. While LS is simple and computationally efficient, MMSE offers better performance by accounting for noise in the channel. MLSE is the most accurate technique but is computationally complex and may not be suitable for real-time applications. The choice of channel estimation technique depends on the specific requirements of the system, including complexity, accuracy, and processing power.

**Table 2.2 Comparison between channel estimation methods**

| | Advantages | Disadvantages |
|---|---|---|
| LS | • Simple | • Not accuracy<br>• Enhancement to noise<br>• Not efficient at low (SNR) |
| MMSE | • Better performance than LS | • It is computational difficult<br>• Not efficient at low (SNR) |
| MLSE | • Better performance than LS and MMSE.<br>• It uses an estimation method rather than an equalizing filter. | • Complex method.<br>• It requires complete information about the channel. |

## 2.7 Deep Learning Algorithm (DL)

Interference caused by a large number of users sharing the same spectrum and time slot creates challenges in accurately detecting signals and estimating channels in NOMA networks [53,54]. With an increasing number of users, conventional signal detection and channel estimation methods can become more complicated and expensive to implement. However, deep learning algorithms provide a solution by identifying the complex correlations between received signals and basic data [55].

Deep neural networks can detect signals and estimate channels even in the presence of interference from multiple users. Various deep learning techniques have been utilized in NOMA systems, including CNNs and RNNs. This section

will discuss in detail the most popular types used in this thesis, as well as our proposed approaches. Figure (2-10) illustrates the architecture of deep neural networks, commonly referred to as DNNs, which are a type of artificial neural network model with multiple hidden layers between the input and output layers. Two of deep learning algorithms which are mostly used in sequence data processing will be explained in the next sections. These algorithms are: RNN (GRU and LSTM) and 1-d CNN.

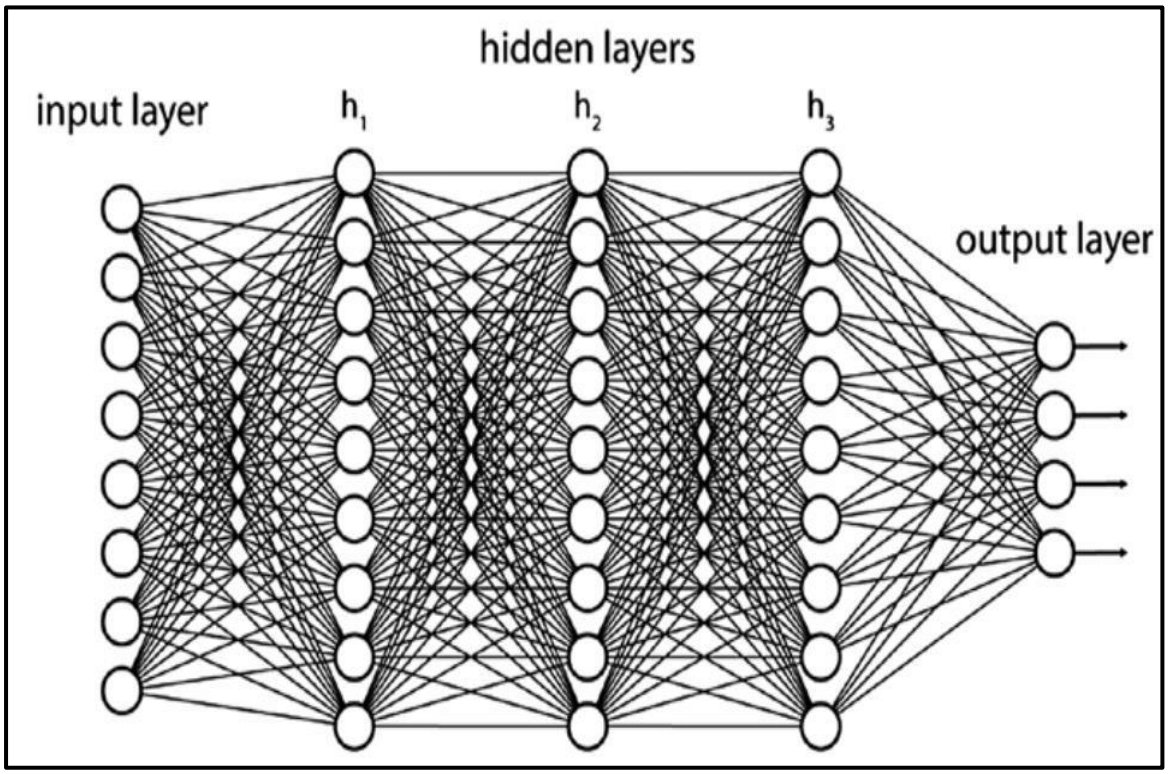


Figure 2-10 Deep neural networks (DNN) [55].

## 2.8 Recurrent Neural Networks (RNN)

One of the most widely utilized deep learning architectures for sequence data is recurrent neural networks (RNNs). They have excelled at challenges involving time series analysis, textual, voice recognition, machine translation, and other sequence-based issues. Yet, they are burdened with the terrible problem of **vanishing gradients**. In simplest terms, as the length of the

sequence lengthens, this network's capacity to remember or retain meaningful information rapidly declines. A specific kinds of RNN called an LSTM and GRU networks works to address this remembering challenge.

### 2.8.1 Long Short Term Memory

In back propagation training algorithm, the long short-term memory (LSTM) largely overcomes the vanishing gradient issue. A gate technique is used by LSTMs to regulate the memorizing procedure. Using gates that open and close, data can be read, written, or saved in LSTMs. These gates provide component multiplication by sigmoid levels between 0 and 1, keeping the memory in analog form. Because it is differentiable, analog is a good choice for back propagation. An LSTM has three distinct gates: an input gate, an output gate, and a forget gate with five activation function (three sigmoid function and two tanh function). Figure (2-11) shows the architecture of (LSTM).

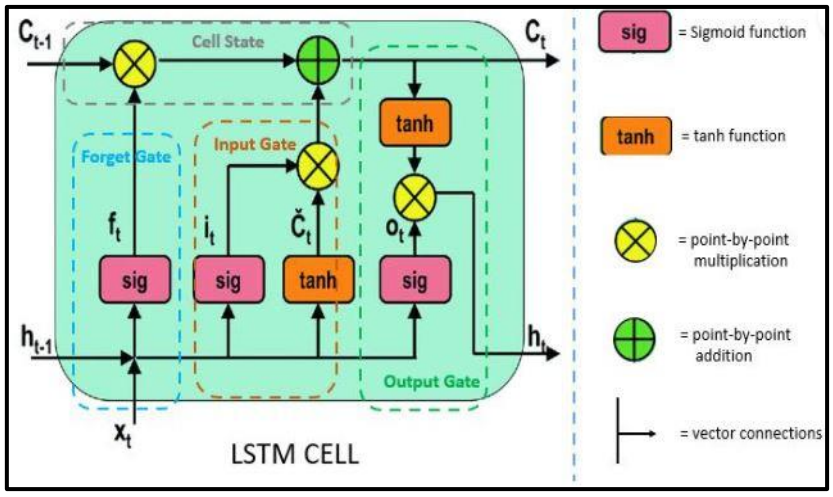


Figure 2-11 The architecture of (LSTM) [56].

#### 2.8.1.1 Sigmoid Function ($\sigma$)

It is one of the most commonly used activation functions that give values in the period between zero and one by applying E.q (2.25). Frequently used in prediction models where the output files are probability dependent, given that

the probability assumes the values within the specified period between zero and one. Figure (2-12) shows the sigmoid activation function, which is in the form of the letter S-shape, starting with zero and ending with one. The sigmoid function is a non-linear function and the prediction accuracy is high in binary classification [57,58].

$$\sigma(\gamma) = \frac{1}{1+e^{-\gamma}} \tag{2.25}$$

Where $\sigma(\gamma)$ is sigmoid function, $y$ is total input to the hidden neuron.

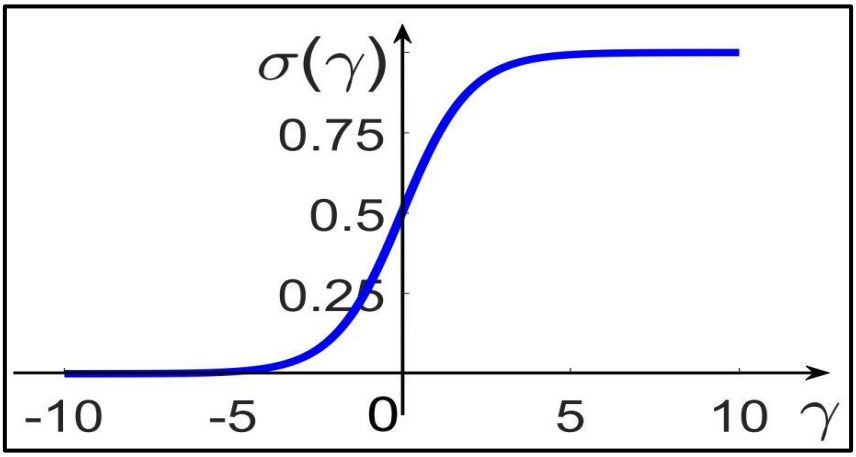


Figure 2-12 Sigmoid function [58].

### 2.8.1.2 Tanh Function

Tanh is an activation function that is not linear. It controls the values moving through the system, keeping them within the range of -1 and 1. A function whose second derivative may exist for a longer period of time is required to prevent information fading. It's possible that some values will grow large, further making other values unimportant. LSTM contains two Tanh functions. Figure (2-13) shows this activation function.

$$\tanh(x) = \frac{e^{x}-e^{-x}}{e^{x}+e^{-x}} \tag{2.26}$$

Where $\tanh(x)$ is tanh function, $x$ is total input to the hidden neuron.

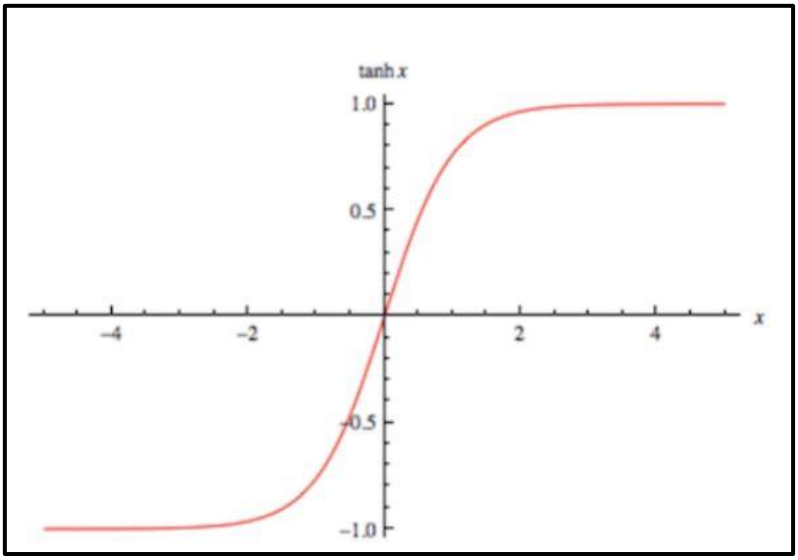


Figure 2-13 Tanh function [58].

### 2.8.1.3 Forget Gate

The forget gate determines what information must be stored and what can be forgotten. The sigmoid function receives data from the current input $x(t)$ and prior hidden state $h(t-1)$. The Sigmoid algorithm generates numbers between 0 and 1. It indicates that some part of the previous output is necessary (making an output that is near 1). The amount of $f_t$ will then is utilized by the cell for one by one multiplication. From Figure (2-11) and eq. (2.27) shows the operation of this gate.

$$f_t = \sigma\left(w_f . [h_{t-1}, x_t] + b_f\right) \tag{2.27}$$

Where $f_t$ forget gate at time step$(t)$ , $x_t$ a feature for input, $h_{t-1}$ prior hidden state, $w_f$ the weighting matrix among the input gate and the forget gate. $b_f$ correlational bias at $(t)$ .

### 2.8.1.4 Input Gate

Referring with Figure (2-11) to modify the cell value, the input gate makes the following actions. The second sigmoid function is first applied to feature input $x_t$ and prior hidden state $h_{t-1}$ as inputs. The values are modified from one or (related) to zero or (not related). The information in $x_t$ and $h_{t-1}$

will then be passed at the tanh function. In order to control the system, the tanh function will create a ($\bar{C}_t$) vector for each possible number between -1 and 1. On the output values formed by the activation functions, one-by-one multiplication can be done. Eq. (2.28, 2.29) shows the operation of this gate.

$$i_t = \sigma(w_i.[h_{t-1}, x_t] + b_i) \quad (2.28)$$

$$\bar{C}_t = tanh(w_c.[h_{t-1}, x_t] + b_c) \quad (2.29)$$

Where $i_t$ input gate at time step$(t)$ ,$w_i$ weight matrix between input gate and output gate. $b_i$ Connection bias at $(t)$ , $\bar{C}_t$ value generated by tanh function , $b_c$ bias vector, $w_c$ weight matrix between cell state information and network output.

### 2.8.1.5 Cell State $(C_t)$

The networks now have adequate information due to the input gate and forget gate. Next comes a decision and save the information from the new state in the cell state. The prior state of the cell $C_{t-1}$ has been multiplied by the forget data vector $f_t$. If the result is 0, values will be eliminated from the cell state. After that, the network performs one-by-one addition on the output value of the vector input ( $i_t$), updating the cell state and supplying the network with a new cell state $(C_t)$.

$$C_t = f_t * C_{t-1} + i_t * \bar{C}_t \quad (2.30)$$

Where $C_t$ cell state information, $C_{t-1}$ prior state of the cell, $\bar{C}_t$ value generated by tanh, $f_t$ forget gate at time step$(t)$, $i_t$ input gate at time step$(t)$ .

### 2.8.1.6 The Output Gate

The output gate determines the outcome of the following hidden state. This state contains information about previous input. The values of the prior hidden state and the current hidden state are first sent to the third sigmoid function. The newly created cell state that was derived from the initial cell state

is then subjected to the tanh function. One by one, these two outcomes are multiplied. Based on the final value, the network decides which information the hidden state should convey. This hidden condition is utilized for predicting. The new hidden state and the new cell state are then carried into the future time step. Can be represented this behavior by the equations below:

$$o_t = \sigma(w_o.[h_{t-1}, x_t] + b_0) \quad (2.31)$$

$$h_t = w_o * tanh(C_t) \quad (2.32)$$

Where $o_t$ the gate output at$(t)$, $w_o$ the matrix weight at the gate output, $b_0$ the vector bias, $h_t$ the final output of LSTM .

**To summarize, the forget gate selects the significant data from the last step that is required. The input gate selects the significant data that can be provided from the present state. The output gate generates the input data for the next state.**

### 2.8.2 Gated Recurrent Unit (GRU)

GRU is a type of gated RNN, which by using a product and process design, significantly reduces the issue of gradient vanishing in RNNs, and simplifies the structure while keeping the effect of LSTM [59]. The Gated Recurrent Unit is the newest current in the sequential model to study, which gives it a distinct advantage over other RNN networks [60]. Long short-term memory and gated recurrent unit are nearly identical. Similar to LSTM, GRU manages information flow utilizing gates. In contrast to LSTM, it only has two gates and doesn't save the interior state of the cells. Data from an LSTM recurrent unit's interior cell state is combined with the hidden state in case we used the gated recurrent unit. The next gated recurrent unit receives this collected data. Below is an explanation of each gate of a GRU. Figure (2-14) show the architecture of (GRU).

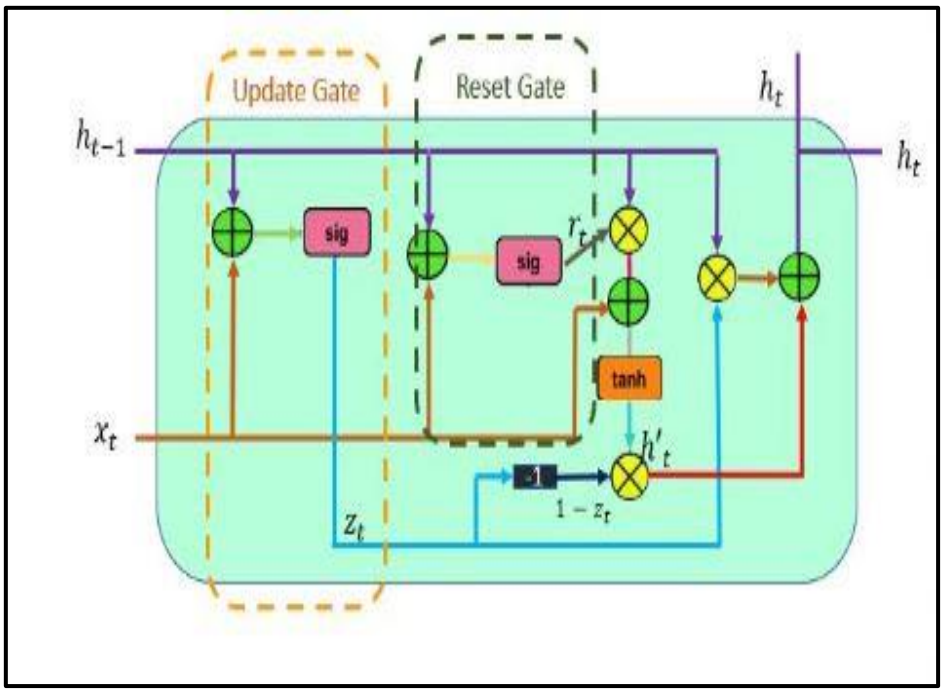


Figure 2-14 The architecture of (GRU) [56].

### 2.8.2.1 The Update Gate

It specifies what percentage of the prior data needs to be passed on in future periods. It is similar to an LSTM recurrent unit's Output Gate. Eq. (2.33) shows the operation of this gate.

$$z_t = \sigma(w_u . [h_{t-1}, x_t] + b_u) \tag{2.33}$$

Where $z_t$ update gate, $w_u$ update gate weight matrix, $b_u$ connection bias at $t$ , $h_{t-1}$ previous hidden state, $x_t$ current state.

### 2.8.2.2 Reset Gate

It decides how much previous information should be forgotten. It is identical for merging the input gate and the forget gate in an LSTM recurrent unit. Eq. (2.34) shows the operation of this gate.

$$r_t = \sigma(w_r . [h_{t-1}, x_t] + b_r) \tag{3.34}$$

Where $r_t$ reset gate, $w_r$ reset gate weight matrix, $b_r$ connection bias at $t$.

### 2.8.2.3 Current Memory Gate ( $h_t$)

It can be calculated as a combination of the prior memory gate $(h_{t-1})$and the candidate activation $(\bar{h}_t)$ at the present time step. $(h_{t-1})$ is integrated into the reset gate.Utilizing a non-linear transformation to the combination of the input vector $(x_t)$ at the current time step and $[(h_{t-1}) \cdot r_t]$, the candidate activation $(\bar{h}_t)$ is calculated.

$$\bar{h}_t = \tanh(w_h.[r_t \cdot (h_{t-1}), x_t] + b_h) \quad (2.35)$$

Where $w_h$ reset gate weight matrix and $b_h$ connection bias at $t$. Finally, add the two vectors to get the currently hidden state vector ( $h_t$).

$$h_t = (z_t \cdot h_{t-1}) + (1 - z_t \cdot \bar{h}_t) \quad (2.36)$$

**Summary the update gate $(z_t)$determines how much of the candidate activation $(\bar{h}_t)$ is used to update the currently hidden state vector( $h_t$), whereas the reset gate $(r_t)$ determines how much of the prior memory gate $(h_{t-1})$ is utilized for calculating the candidate activation$(\bar{h}_t)$. These gates permit the GRU effectively update its memory and store significant data over time.**

## 2.9 1-d Convolutional Neural Networks (1-d CNNs)

The one-dimensional convolutional neural network is commonly referred to as 1D CNN. It is a specific kind of neural network that is usually applied to analyzing time series data or one-dimensional signals, by sequential data. While traditional convolutional neural networks (CNNs) function on 2-d images, 1-d CNNs use one-dimensional input data [61]. A group of filters are applied to the input data of a 1D CNN for the purpose to extract features important to the task at hand. The convolutions performed at each stage by these filters as they move along the input signal result in a collection of feature maps that represent various aspects of the input information. The feature maps are then fed into

several layers that work out operations like pooling and non-linear activation, after which they are passed to a final output layer that generates the network's estimation. The pooling layer reduces the dimensionality of the feature maps in contrast the non-linear activation function adds non-linearity to the system, enabled of keeping complex connections between the input and output. The structure of a 1-d CNN can present in Figure (2-15).

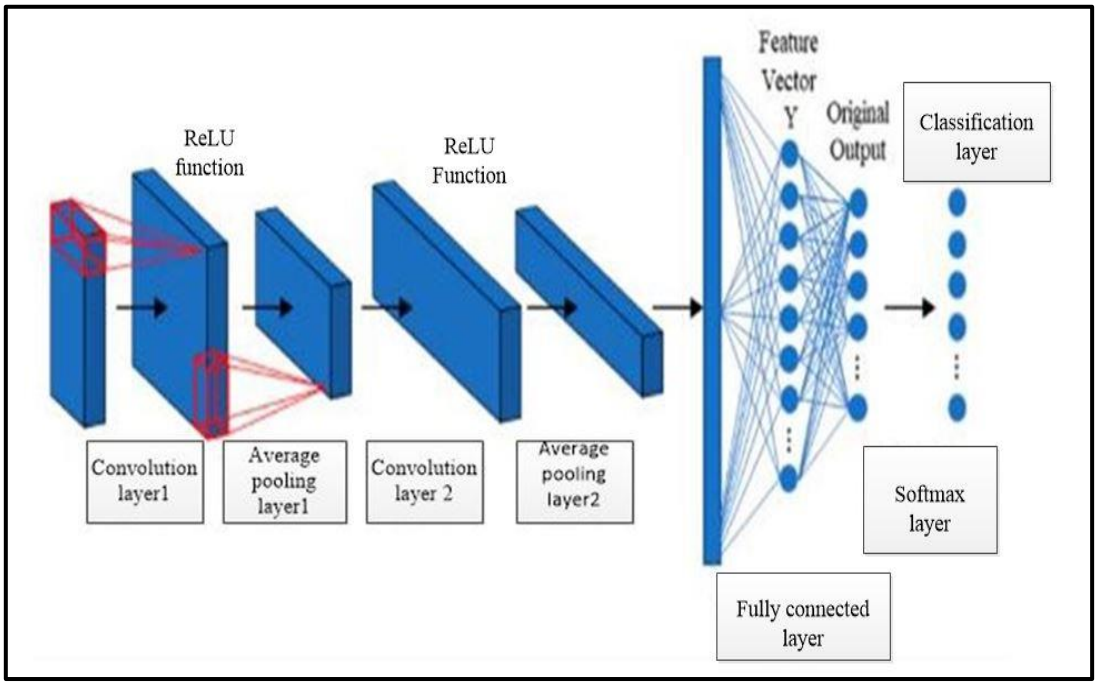


Figure 2-15 The architecture of (1-d CNNs) [62].

## 2.9.1 Convolution Layer

It is the first layer through which features are extracted by the convolution process. Convolution layers contain a large number of digital filters. Using the convolution process turns the input into new shape called feature maps. Feature maps show the salient features of the input. The convolution layer is distinguished from the rest of the CNN layers by its use of filters instead of weights, each convolution layer filter creates a single feature map. Convolution filters are one-dimensional. Through training, filter matrix values are

determined in a similar way to updating weights in simple neural networks, the convolution filter values are constantly updated throughout the training phase [63]. The number of outputs of the feature map ($O_F$) can be calculated from Eq. (2.37).

$$O_F = \frac{X_p - F + 2P_a}{S} \tag{2.37}$$

Where $X_p$ number of input feature, $F$ size of filter, $P_a$ the amount of padding, $S$ is stride (stride is the number of steps the kernel moves over the original input sequence) [64]. The equation for one-dimensional convolutional neural networks (CNNs) involves the convolution operation between the input signal and the convolution kernel, followed by a non-linear activation function. Assuming an input signal x of length p and a convolution kernel w of length k, the output y of a one-dimensional CNN can be computed as Eq.(2.38)

$$Y(\mathrm{i}) = \sigma\left(\mathrm{b} + \sum_{\mathrm{j}=0}^{\mathrm{k}-1} \mathrm{w(j)} * \mathrm{x(i+j)}\right) \tag{2.38}$$

Where $Y(\mathrm{i})$ is the i-th element of the output signal, b is the bias term, σ is the activation function, j represents the position of the kernel element that is multiplied with the input signal element at position (i+j) during the convolution operation. Figure (2-16) shows the steps involved in a convolutional network with a 3-K kernel size.

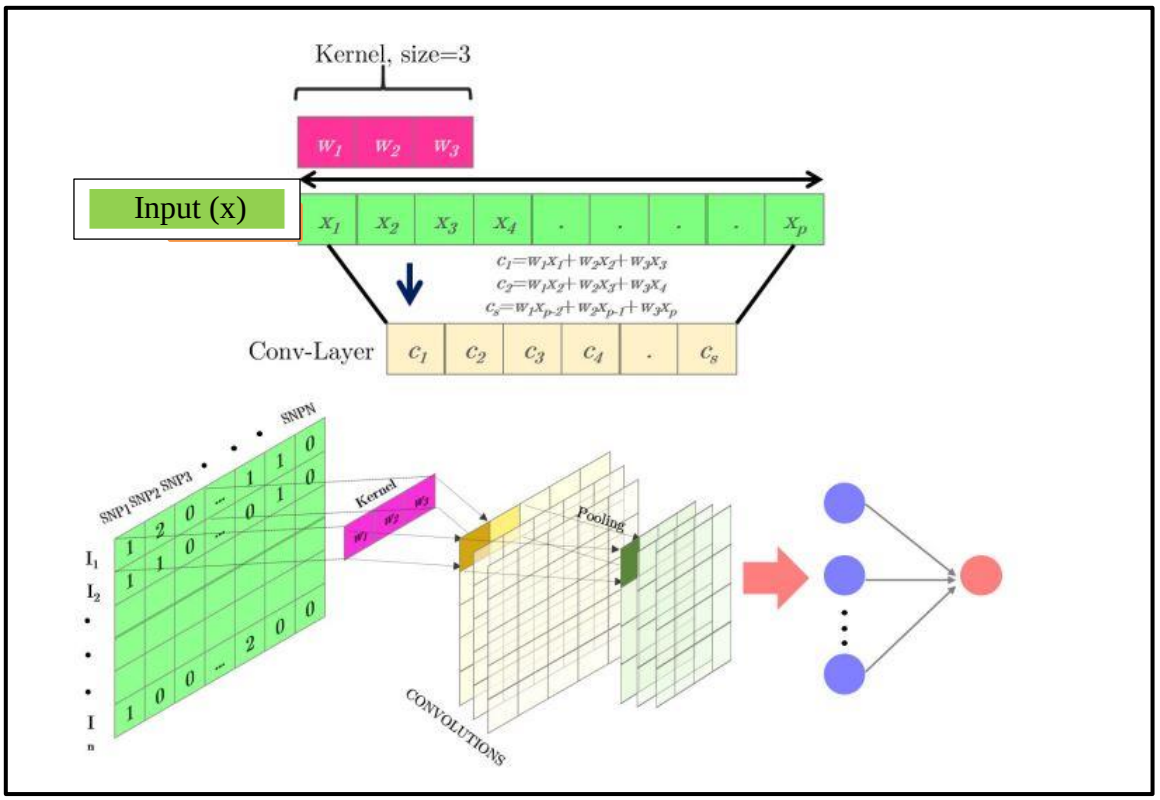


Figure (2-16) The operation of a 1-d convolutional layer [63].

## 2.9.2 Average Pooling Layer

It is the second layer of 1-d CNN, it is use to compress the output of the convolutional layers into a single feature vector. For each group that relates to the classification assignment in the final Conv layer, one feature is created. It takes the average of each feature map and feeds the resulting vector straight into the (softmax) layer rather than putting fully connected layers on top of the feature maps. To calculate the average pooling ($\rho_{av}$), the E.q (2.39) is used.

$$\rho_{av} = \frac{\sum a_i}{N} \tag{2.39}$$

Where $N$ is number of feature map, $a_i$ the values of the feature map in the input array.Figure (2-17) presened average pooling layer.

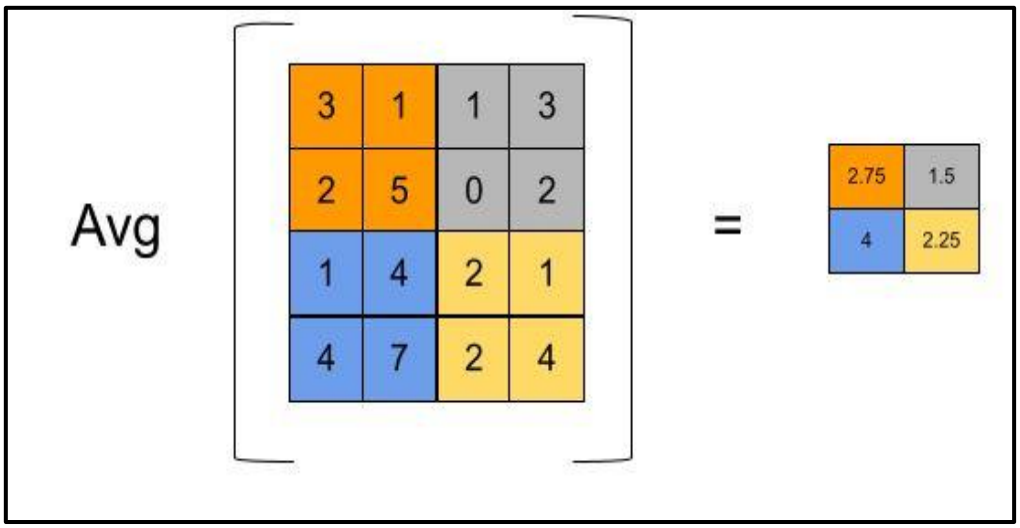


Figure (2-17) The resultant of the average pooling layer [65].

### 2.9.3 Activation Layer

After the convolution layer, the features are entered into the activation layer. There are many different kinds of activation functions and they all pass complex features. Activation functions allow the information to be transmitted to the next neuron, and the activation layer is always between two layers of CNN. Figure (2-18) presents the general structure of the activation function in the fully connected (dense) layer .

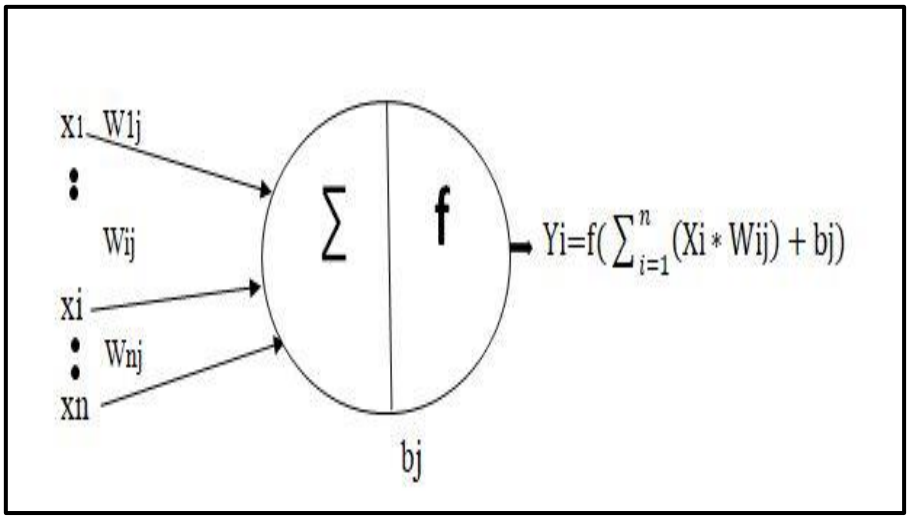


Figure (2-18) General activation function structure [66].

Where: xi represents the input feature, j at the same time, n features are input to the neuron, bj represents the internal state of the neuron j, wij represents the weight value of the connection between the input feature xi and the neuron j, and Yi is the output of the neuron j. f (•) is the activation function [56]. In the previous section, we dealt with two types of this activation function (sigmoid and tanh), here we will take others types such as rectified linear unit (ReLU) and Softmax Function.

### 2.9.4 ReLU Function

ReLU is a standard and powerful feature of deep learning networks. The output of the ReLU is a nonlinear function, the principle of action of the ReLU is shown in the mathematical expression in equation (2.40). The f(x) of the ReLU will be zero for all x-values less or equal than zero and the f(x) will be x for all x-values greater than zero. Figure (2-19) show the ReLU function [67].

$$\text{ReLU}(x) = \max(0, x) = \begin{cases} x, & if \;\; x > 0 \;\; Active \\ 0, & if \;\; x \leq 0 \;\; Inactive \end{cases} \qquad (2.40)$$

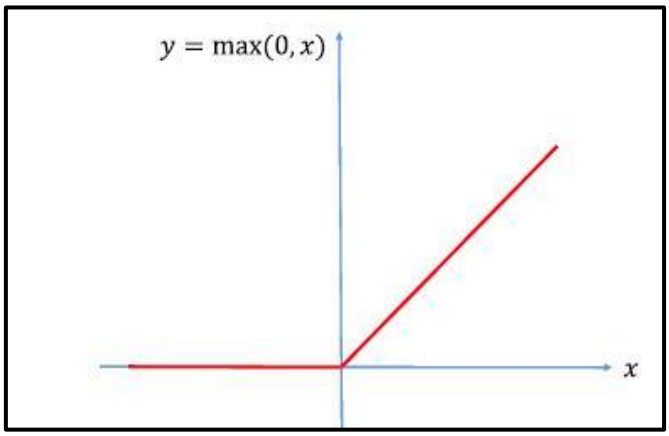


Figure (2-19) The ReLU function [67].

### 2.9.5 The Softmax Function

It is an activation function frequently used in deep neural networks. It is a generalization of the sigmoid function and it is nonlinear. The Softmax function is widely used in multi classification, so it is used in the outer layers of deep

neural networks, all output values of the Softmax function are between zero and one, so it expresses the probability. It is used in the output layer to convert the product of linear values into a probability product between zero and one, by applying E.q (2.41) [68].

$$\sigma(x_c) = \frac{e^{x_c}}{\sum_{j=1}^{C} e^{x_j}} \tag{2.41}$$

Where $c$ represents the number of classes, $x$ is a C-dimensional input vector with arbitrary real-values. Figure (2-20) shows the softmax function and how to classify when the output is categorical [69].

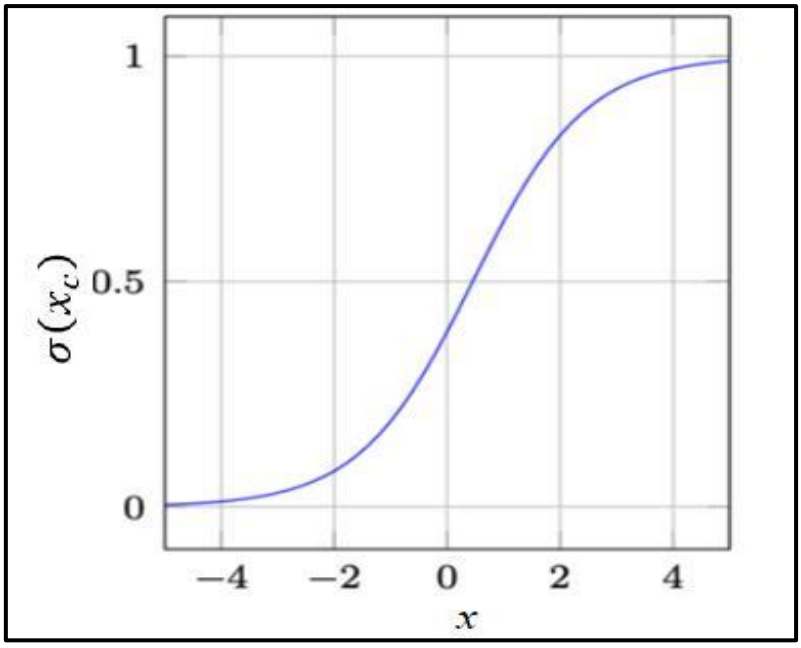


Figure (2-20) Softmax function [69].

## 2.9.6 Fully Connected Layer (Fc)

The output should be converted to a vector of probabilities using a fully connected layer with a data size equal to the number of classes. The output of the fully connected layer is adjusted to the density function of probability over the output labels by the Softmax layer.

### 2.9.7 Classification Layer

The classification layer is the final layer in a neural network responsible for generating output predictions. Its primary purpose is to produce a probability distribution across the potential classes or labels for a given input. It transforms the network's raw output into meaningful class probabilities, facilitating decision-making in tasks like image classification, natural language processing[69].

# CHAPTER THREE

# Proposed Model

# CHAPTER THREE

# Proposed Model

## 3.1 NOMA-OFDM Hybrid System

OFDM is a promising solution for use in NOMA systems due to its ability to mitigate inter-user interference and permit sharing of the same frequency band with many users. Through dividing the spectrum into various subcarriers, OFDM enables parallel transmission of multiple users on different subcarriers, reducing inter-user interference and improving overall system performance. Hybrid NOMA-OFDM systems provide even more flexibility by allocating power to each user in the power domain and then dividing the available spectrum into subcarriers using OFDM to transmit data in parallel. This efficient use of available spectrum improves the system capacity and spectral efficiency.

However, the complexity of the hybrid NOMA-OFDM system can increase due to nonlinear distortions caused by fading, interference, and noise, and a large number of users, subcarriers, and network conditions. To address this challenge, deep learning can provide accurate, efficient, and adaptive signal detection and channel estimation to improve system performance, spectral efficiency, and utilization of the available spectrum.

Our investigation suggests using GRU and 1-dCNN, two new DL architectures, for NOMA-OFDM systems' signal detection and estimation of channel. These architectures have not been used before in this context, and in the next chapter, we will demonstrate the strengths and advantages of our proposed systems. Through experiments and simulations, we aim to show that our DL-based NOMA-OFDM approach can outperform traditional SIC-based techniques and state-of-the-art DL-based algorithms. Our work has the potential to improve the performance, spectral efficiency, and utilization of available spectrum in

NOMA-OFDM systems, leading to more efficient and effective communication networks.

## 3.2 The Proposed System

In the literature, there are several DL systems that have been proposed and implemented to enhance NOMA signal detection in terms of SER. However, in real-time scenarios, more efficient systems are required to reduce errors and increase the speed of training and testing for the DL approach.

In this work, we propose two new DL architectures for signal detection in NOMA-OFDM systems. Firstly, we propose to use a new type of RNN gate recurrent units (GRU), which will be trained at different signal-to-noise ratios to detect communication signals. We will compare the performance of the GRU with other DL structures, such as as Long Short Term Memory (LSTM) and Bi-directional(BILSTM), and state-of-the-art techniques such as Least Squared Error (LS),Mean Sqeared Error (MMSE), and Maximum Liklihode (ML), in terms of Signal to Noise Ratio(SNR).

Secondly, we propose a unique type of CNN, namely one-dimensional convolution network (1-d CNN), which will also be trained at different signal-to-noise ratios to detect communication signals. Similarly, we will compare the performance of the 1-d CNN with other DL structures such as (LSTM), (BILSTM), and proposed (GRU), as well as with state-of-the-art techniques such as LS, MMSE, and ML, in terms of (SNR).

Furthermore, we will investigate the effect of reducing the length of cyclic prefix (CP), the number of pilots, and the increased number of multipath on the system. We will make a comparison between the proposed models with other deep learning systems and traditional methods.

Finally, we will calculate the time required for training the suggested systems and show that the proposed systems are faster than the other DL models under any given scenario. Through our experiments and simulations, we aim to

demonstrate the strengths and advantages of our proposed systems and prove that they have the potential to outperform existing DL-based and traditional techniques. Our work can lead to more efficient and effective communication networks with improved performance, spectral efficiency, and utilization of available spectrum in NOMA-OFDM systems.

## 3.3 Structure of The Proposed Model

In this thesis, we used two user-equipment (UE) hybrid uplink NOMA-OFDM system with one base station representing a receiver to detect superposing signals from two user-equipment (UE) and used the proposed (GRU and 1-dCNN) systems to aid NOMA- OFDM signal detection and channel estimation from one operation. Figure (3-1) present the two-user uplink NOMA system.

In an OFDM framework with 64 subcarriers, the information is sent as OFDM packets, where each packet contains three OFDM symbols. Every (UE) is given one pilot symbol in the first two OFDM symbols of each packet, and one data symbol in the third OFDM symbol combines the data symbols from two UE. The far user (FU) has a bad channel condition with a high power allocation coefficient (0.9760) transmitted signal $x_1$ and the near user (NU) has a high channel condition with low power allocation coefficient (0.0240) transmitted signal $x_2$.The transmitter and receiver have a known CSI for power distribution. The idea of power distribution is to give several users a reasonable SINR for cooperative decoding at the receiver.

By transmitting the pilot symbols with a random phase shift, the receiver can estimate the channel response and correct for any frequency and phase offsets that may be introduced during transmission. Each symbol in the quadrature phase shift keying (QPSK) modulation has two bits per subcarrier. As a result, one out of 16 possibilities could apply to the sent bits from both users if the

symbols produced by the two users are transmitted together. Figure (3-2) show the proposed system. Where every user Performs an inverse FFT to convert the symbols into the time domain, inserts the cyclic prefix, and converts the parallel signal into a serial signal, the OFDM packet was carried over the Rayleigh channel where the signals multiplies with the channel frequency response and adds complex Gaussian noise. Considering the superposition of N users on sub - carriers K, The amplitude of the received data at base station (BS) can be estimated in the frequency response given in Eq. (3.1)[10].

$$Y(k) = \sum_{n=1}^{N} \sqrt{P_n(k)}\ H_n(k)x_n(k) + W_n \qquad (3.1)$$

Where: $Y(k)$ Frequency response of received data and $x_n(K), W_n$ is information transmitted from user $(n)$ and the white additional noise with a mean and variance $W_n \sim W(0, \sigma^2)$ accordingly. $P_n(k), H_n(k)$ the transmitted power for each user $(n)$ and Fast Fourier transformation (FFT) of an impulse response from a multipath channel $\left(h_n(t)\right)$ accordingly it is given in Eq. (3.2)[10].

$$h_{\mathrm{n}}(t) = \sum_{l=1}^{\mathrm{L}} \rho_{n,l}\ \delta\left(\mathrm{t} - \tau_{n,l}\right) \qquad (3.2)$$

Where $\rho_{n,l}$ and $\tau_{n,\mathrm{l}}$: The complicated channel gain and the equivalent delay in time of the $l$ th component for user $(n)$ with multiple paths respectively.

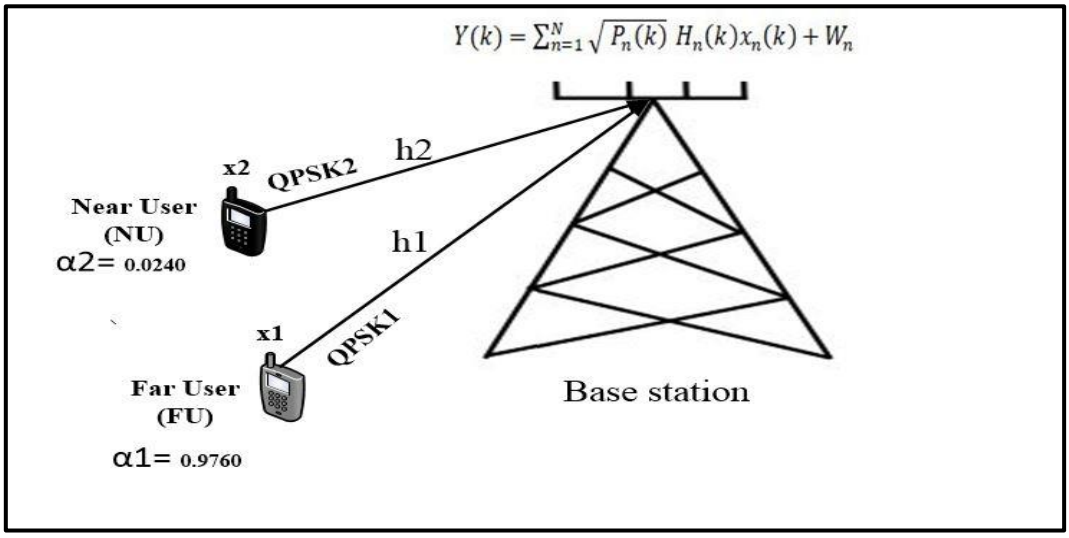


Figure 3-1 Two user and a single base station uplink NOMA system.

The Rayleigh fading channel with a finite number of paths $l$ is 20 and the total delay that represents guard is 20. This guard must not be shorter than $l$ to avoid a situation (ISI). At receiver removes the cyclic prefix, performs an FFT to convert the signal back into the frequency domain, and returns the receive packet and random Phase.

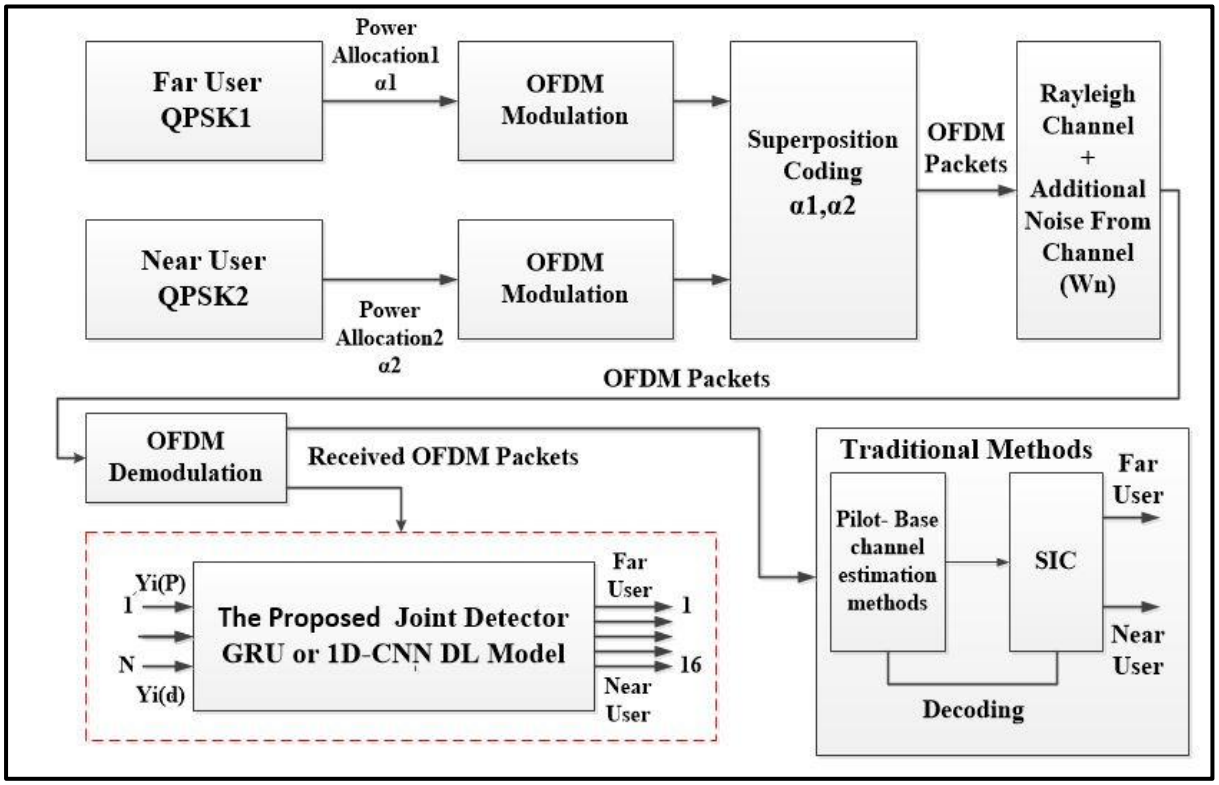


Figure 3-2 The proposed DL based NOMA-OFDM estimation system.

## 3.4 SIC With Channel Estimation Methods

To prove the proposed models outperform the traditional channel estimation methods (CE) we need to perform SIC and (CE) to detect signals at the receiver. The received signal separates into two streams, corresponding to the strong user and weak user, respectively. However when the single base station antenna receives coupled signals ($x_1$,$x_2$), decode the data from the near user ($x_2$) first with the low power, along with the noise channel ratio and the power to interference power from many other users for the user $n$ where $n$ not equal to 2 is given by Eq. (3.3)[21].

$$\mathrm{SINR}_2 = \frac{E\alpha_2|h_2|^2}{E\sum_{n\neq 2}^{N}\alpha_n|h_n|^2+1} \quad (3.3)$$

Where: $h_n$ and$\alpha_n$: the various fading channels condition and power allocation coefficient of user $(n)$ respectively, $E$ the ratio of signal to noise given by Eq. (3.4)[10].

$$E = \frac{P}{\delta^2} \quad (3.4)$$

Where: $\delta$ and $P$: The variation in noise and the sum of all user power respectively. $\alpha_n$ Power allocation factor with user $(n)$ it is given in Eq. (3.5)[10].

$$\sum_{n=1}^{\mathrm{N}}\alpha_n = 1 \quad (3.5)$$

Then the SINR for user 1 can be given in Eq. (3.6)[21].

$$SINR_1 = E\alpha_1|h_1|^2 \quad (3.6)$$

Finally, the sum rate for all users at a base station is given by Eq. (3.7).

$$R_{SUM} = log_2(1 + E\sum_{n=1}^{N}\alpha_n|h_n|^2) \quad (3.7)$$

From (SIC) method the far (user1) depend on near user (user1) since imperfect SIC will be generate error in signal detection therefore we need to make channel estimation before SIC algorithm.In this thesis used most common traditional methods such (LS,MMSE and ML) and compared it to proposed DL models.

**LS:** extracts the pilot symbols and data symbols for each user, and calculates the LS channel estimate based on the received data and pilot symbols. Then it performs interpolation to estimate the channel response at all subcarriers.

**MMSE:** extracts the pilot symbols and data symbols for each user and it uses the channel correlation matrix and the noise variance to calculate the MMSE channel estimate. The MMSE filter takes into account the interference from the other users in the system.

**ML:** this method considering perfect channel prediction by computing all possible transmitted data based on the QPSK symbols and the power allocated factor for each user and packet. It computes all possible received data by multiplying the transmitted data with the channel coefficients and the random phase shifts for each user and packet. The received signals from both users are then added up to obtain the total received signal. ML then computes the mean square error between the received signal and each possible transmitted signal. It then finds the index of the transmitted signal that has the minimum mean square error. Using the index of the transmitted signal, the ML algorithm obtains the label for the estimated symbol for each user and packet. It then computes the error rate by comparing the estimated labels with the transmitted labels for each user. Finally, it returns the error rate and the estimated labels for the transmitted symbols for each user and packet. Figure (3-3) presented this.

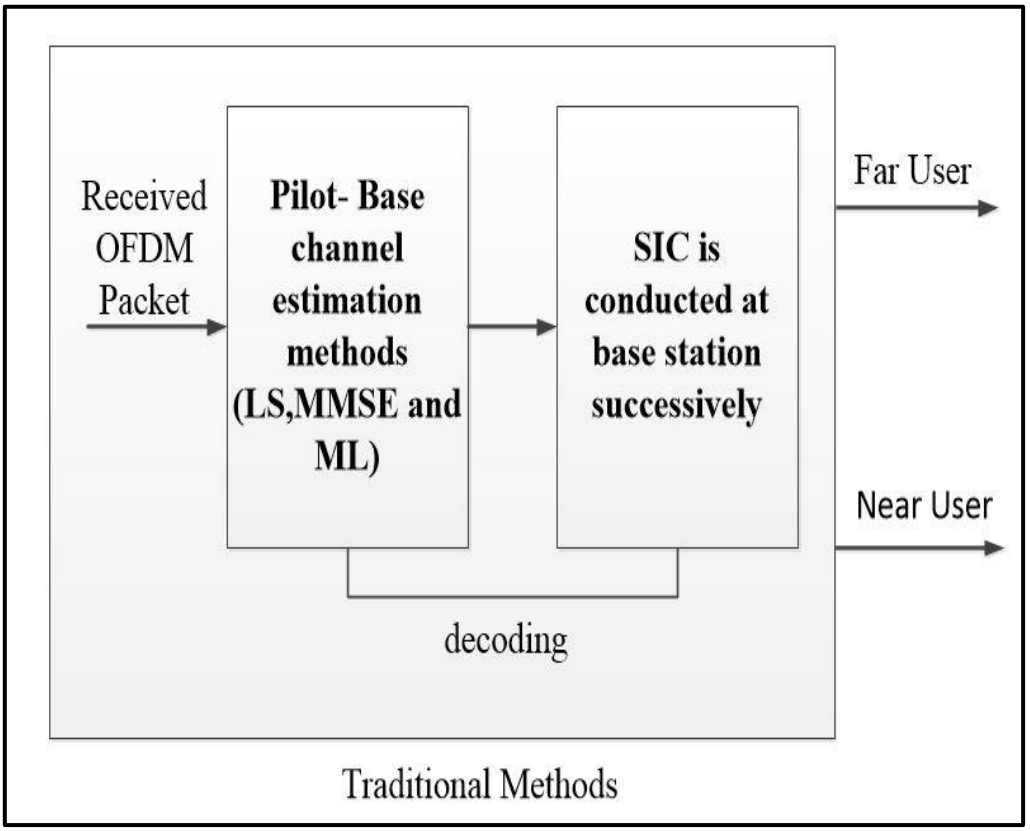


Figure 3-3 Pilot-based channel estimation and SIC detector

## 3.5 The Proposed Joint Detector DL Model

The received OFDM packets are being used as training data for deep learning (DL) in order to integrate channel estimation and Non-Orthogonal Multiple Access (NOMA) signal detection in a single process. The essential assumptions each OFDM packet consists of three symbols - two pilot symbols and one data symbol. QPSK modulation is being utilized, which means each symbol can take one of four possible values. Since there are two users in the system, the total number of label combinations can be calculated as $4^2 = 16$. The DL is trained assuming a static channel, which means the channel characteristics remain constant during training.

The training process assumes a specific number of pilot subcarriers, a specific length of cyclic prefix, and a specific number of propagation paths, these parameters define the characteristics of the simulated channel. To test the robustness of the DL model, a random phase shift is added to each packet. By training the neural network on this data, it is expected to learn the relationships between the received signals and the corresponding symbol combinations. This enables it to accurately detect and decode the symbols transmitted by each user, even in the presence of channel variations introduced by the random phase shifts or change some important parameters.

### 3.5.1 Data Generation of Proposed DL Model

Feature vector (Yi) created from the received OFDM packet and used to preserve it as a sample for the training set. It will use this feature vector (real + imaginary) to generate training data in the form of input-output pairs for a neural network to learn the pattern between the transmitted signal and the received signal. Figure (3-4) show the received OFDM packet. The feature set (Yi) consists of real and imaginary values of each symbol in the OFDM packets. The input size for training(x train) is 64 multiplied by 3 × 2= 384. In this work

the label is a number range of 1 to 16 and the number of packet class is $1e^4$ then you will have 16 classes and each class will have 10000 samples, so the total number of training samples in the dataset will be $16 \times 10000 = 160000$ samples and this represented ( y train label ) to train the deep neural network system. The training data is divided into smaller batches. Each batch contains a subset of training samples. One iteration involves processing a batch through the Deep Neural Network (DNN) with both forward and backward passes. In this study, it takes 8 such iterations to complete one cycle of processing the entire training dataset, which is referred to as an epoch.

The Target subcarrier for signal detection is index 20 from 64 index subcarrier on each packet and target signal-to-noise ratio for FU and NU is 12dB.Where FU has a high power allocation coefficient (0.9760) and NU has a low power allocation coefficient (0.0240) . The generated data samples are separated into two parts: training data size and validation data size. Training data samples are 0.8, about 128,000 samples while validation data samples are 0.2, approximately 32,000 samples.

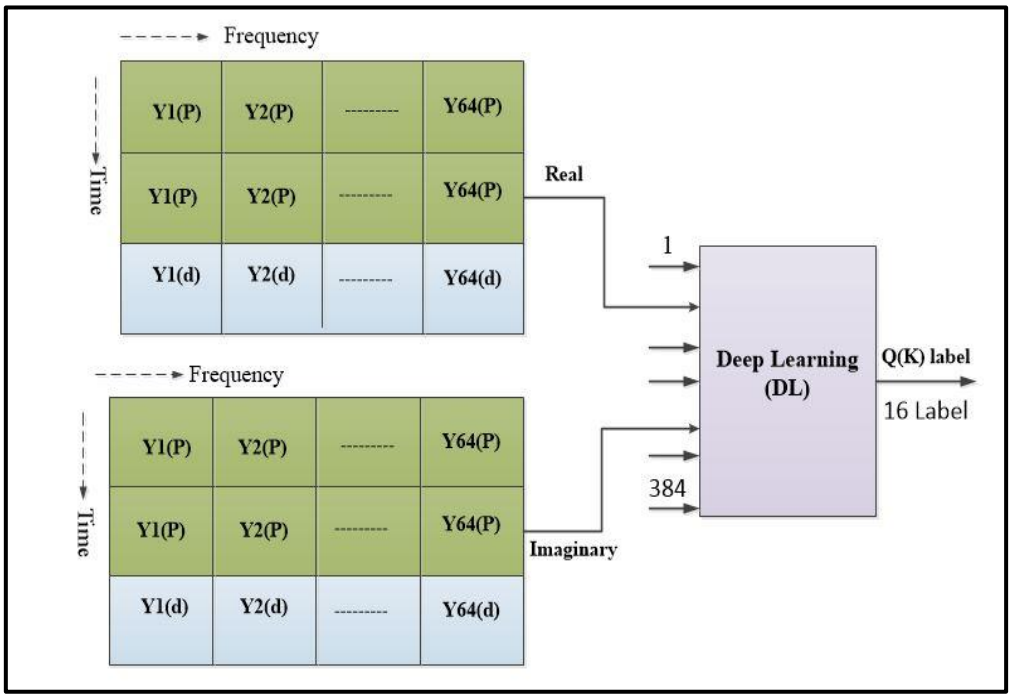


Figure 3-4 Received OFDM packet for training.

## 3.6 The Proposed Joint Detector Based DL-GRU Model

Gated recurrent unit (GRU) is a newer type of RNN that has update gates and a reset gate. The proposed approach utilizes (DL) gate recurrent units (GRU) algorithm to cancel the effect of vanishing or exploding gradients that are affected by other DL algorithms such as recurrent neural networks. We will start the neural network training using the training data. The architecture of the neural network consists of three hidden unit layers of 64, 64, and number of subcarrier units, respectively.

The layers include: a sequence input layer over a dimension that matches the size of the input feature (384), a gated recurrent units (GRU) layer contains 64 hidden units layer, and the fully connected layer with a number matches the number of label classes (16), the softmax layer, and a layer for classification. The input feature (real, imaginary) enter to input layer, this layer sequences the inputs in time steps then the output of this layer is pushed into the modification GRU layers where a choice of the number of hidden units is very important to reduce the overfitting of the deep learning system. In this thesis, we adjusted the GRU layer to 64 hidden units because at this value we obtained high testing accuracy. Figure (3-5) show the proposed joint detector based DL- GRU systems. GRU layer utilizes the update gate to specify how much of the previous data must be transmitted into the future and the reset gate to decide how much previous information should be forgotten.

Fully-connected layer takes the output of GRU layers and converted it to a vector of probabilities with a data size equal to the number of classes (16 label class). The Softmax layer modifies the output's fully connected layer's probability density function over the output labels. The classification layer then produces a highly probable label class.

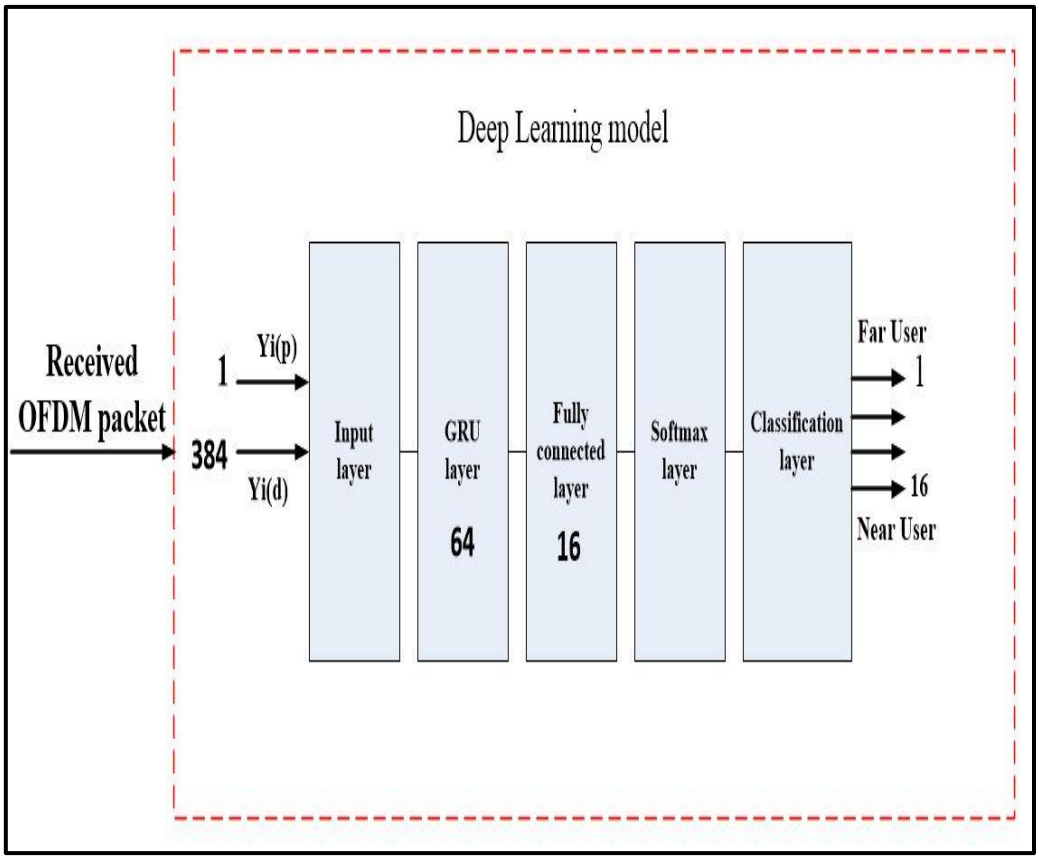


Figure 3-5 The proposed DL - GRU detector.

## 3.7 The Proposed Joint Detector Based DL-1d CNN Model

Another kind of deep learning was proposed in this thesis which is one-dimension convolution neural networks (1-dCNN ) are one of the types of CNN, 1-d CNN was recently used in medical applications, as well as identifying cracks in metallic structures, due to their high training speed compared to other RNN types and high detection accuracy. The reason for this potential is 1-d CNN not used time dependencies to classify data. In this section, we proposed 1-d CNN to aid signal detection in the NOMA-OFDM system. Figure (3-6) show the proposed joint detector based DL- 1dCNN systems.

The suggested system contains two sets of 1- dimension convolution layer and ReLU layer flowed by global average pooling, Softmax layer and fully-connected layer, and classification layer. The convolution layer builds from 32

filters with size 3 and a stride is 2. The input features are converted into new forms called feature maps by the one-dimensional convolution layers. To calculate the output size after each convolutional layer, we can use the Eq. 3.8.

$$Output\ size = \left[\frac{X-F}{S}\right] + 1 \quad (3.8)$$

Where $X$ size of the input sequence, $F$ filter size and $S$ stride size

In this thesis the value of input sequence is 384and then the output for first convolutional layer and second convolutional layer can be present in E.q below.

$$Output\ size_1 = \left[\frac{384-3}{2}\right] + 1 = 191 \quad (3.9)$$

$$Output\ size_2 = \left[\frac{191-3}{2}\right] + 1 = 95 \quad (3.10)$$

The performance of 1-dCNN can be improved by tuning the filter size , number of filters and stride size for every set of convolution layers .In this work, we adjusted the filter parameter to the values we mentioned at the beginning of this section to obtain high testing accuracy. The output of convolution layers enter to the rectified linear unit (ReLU) activation function to generate non linear output value depended on the feature greater or less than zero. However, the (ReLU) lies between two convolution layers.

The global average pooling layer is the second layer of 1-dCNN, this layer is utilized to reduce the output of the convolutional layers into a single feature vector by taking the average for every feature map. Applying a global average pooling layer to the output of a convolutional layer will typically reduce the spatial dimensions to (1x1) while preserving the number of feature maps.

Fully-connected layer (FC) process the output of the global average pooling layers and converted it to a vector of probabilities with a data size equal to the number of classes (16 label classes). The Softmax layer modifies the output's fully connected layer's probability density function over the output labels. The classification layer performs the final classification of the input data into one of the number of classes output classes based on the output probabilities from the

softmax layer. It computes the cross-entropy loss between the predicted and true class probabilities and back propagates the error to update the network parameters during training.

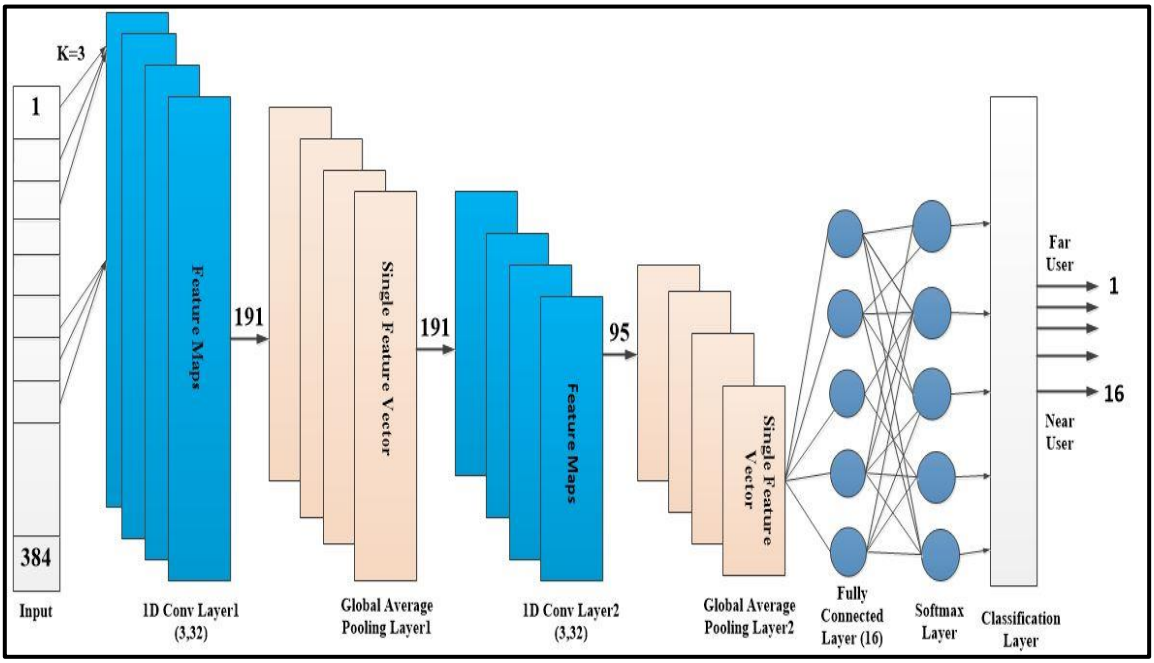


Figure 3-6 The proposed DL – 1-dCNN detector.

# Chapter Four

# Results and Discussion

# Chapter Four

## Results and Discussion

## 4.1 Introduction

In this chapter, the simulation study's findings on suggested DL methods for signal detection in a two-user NOMA-OFDM system are described. The assessment is based on the symbol error rate (SER) as a portion of the signal-to-noise ratio (SNR) for different SNR values between 4 dB and 18 dB with a step of 2dB. This type of simulation study is commonly used in the field of communication systems to assess the performance of proposed signal detection algorithms under different operating conditions such as cyclic prefix (CP), pilot subcarrier number, and multipath number. To increase the reliability and effectiveness of wireless communication systems, deep learning methods for signal detection in NOMA-OFDM systems are an important subject for research. Also comparing the training time of the proposed deep learning system with other existing deep learning systems is a useful way to evaluate its computational efficiency and identify potential areas for improvement. This comparison can also provide insights into the scalability and practicality of the proposed system for real-world applications.

## 4.2 Simulation System Parameters

To ensure fairness in comparing the proposed models (GRU and 1-d CNN) with state-of-the-art [11], [13] standardized the parameters used in the simulation process. Table 4.1 shows the simulation setups. To optimize the proposed model's performance, must perform tweaking and tuning by modifying one parameter while maintaining the others at their original values, and exploring the impact on accuracy for training. Tables 4.2, 4.3 present the tuning parameters.

**Table (4.1): Simulation Setup**

| Parameter | Value |
|---|---|
| Tool for modelling | Toolbox for deep learning in matlab |
| Form optimization | Adam |
| Subcarriers OFDM number | 64 |
| Number of pilots | 64,16 |
| Cyclic prefix (CP) | 20,12 |
| Number of path | 20,30 |
| Channel type | Statical Rayleigh channel |
| Number of NOMA user | 2 |
| Target SNR1 | 12 |
| Target SNR2 | 12 |
| Number of packets | 10000 |
| Batch size requirement | 20000 |
| Epochal duration | 100 |
| Rate of learning | 1% |
| GRU layers | 64 |
| Filter size of (1-dCNN) | 3 |
| Convolution layer (1-d CNN) | 32 |
| Stride size | 2 |

**Table (4.2): Tuning process of GRU layers**

| Test NO. | NO. of GRU layer | Training accuracy (%) | Validation accuracy (%) |
|---|---|---|---|
| 1 | 16 | 75.62 | 68.433 |
| 2 | 32 | 92.335 | 89.24 |
| **3** | **64** | **95.9607** | **95.7** |
| 4 | 128 | 98 | 97.68 |

It's clear from Table (4.2) when the GRU layer is 64 the accuracy difference between training and validation is extremely small, which implies suitable generalization potential and low overfitting.The validation accuracy in test number 4 has a high difference with the training accuracy as compared to test number 3, it indicates a high overfitting and low robustness of DL system.

**Table (4.3): Tuning process of 1-dCNN layers**

| Test NO. | No. of 1D-CNN layers | Filters NO. | Filters size | Stride size | Training accuracy (%) | Validation accuracy (%) |
|---|---|---|---|---|---|---|
| 1 | 1 | 32 | 7 | 2 | 62.326 | 56.1 |
| 2 | 2 | 32 | 7 | 2 | 94.255 | 91.89 |
| **3** | **2** | **32** | **3** | **2** | **92.1424** | **92.1403** |
| 4 | 2 | 64 | 3 | 2 | 96.639 | 95.20 |
| 5 | 2 | 16 | 3 | 2 | 86.593 | 83.557 |
| 6 | 2 | 64 | 5 | 2 | 96.574 | 93.62 |
| 7 | 2 | 64 | 7 | 2 | 96.7424 | 94.664 |
| 8 | 3 | 32 | 7 | 2 | 94.6183 | 92.84 |
| 9 | 3 | 64 | 7 | 2 | 96.917 | 94.23 |

Table 4.3 shows a very small difference between the training accuracy and validation accuracy in test number 3, it suggests that the model has good generalization and high reliability. In this case, selecting the parameters from this test can be a reasonable choice.

## 4.3 Performance Results of Proposed Models

The provided section compares the proposed GRU algorithm with pilot-based channel estimation methods in a perfect case scenario. In this scenario, the number of multipath is 20, the cyclic prefix is 20, and the pilot length is 64. The comparison is based on the performance of different algorithms at various signal-to-noise ratios (SNR) by computing testing accuracy $= \frac{\boldsymbol{correct\ symple}}{\boldsymbol{total\ symple}}$ .

For user 1, the least squared error (LS) method has the worst performance at low SNR. However, its performance improves after reaching an SNR of 16dB, though it still does not meet the required level of performance. The minimum mean squared error (MMSE) method performs better than LS but still has a high error rate at low SNR. The maximum likelihood (ML) method outperforms LS and MMSE, even at low SNR. The proposed GRU algorithm, outperforms the pilot-based channel estimation methods even at low SNR. It outperforms ML by

approximately 2dB until reaching an SNR of 15.7dB, where ML performance becomes identical to the proposed model. These findings also apply to the second user. Furthermore, the proposed GRU model outperforms other (DL) systems with the same channel conditions and system parameters mentioned in references [11] and [13]. It outperforms the DL system in [11] by approximately 2dB and the DL system in [13] by approximately 3dB. Figures (4.1.a and 4.1.b) illustrate the comparisons the proposed GRU algorithm to pilot-based channel estimation methods and the other DL systems in the literature review section.

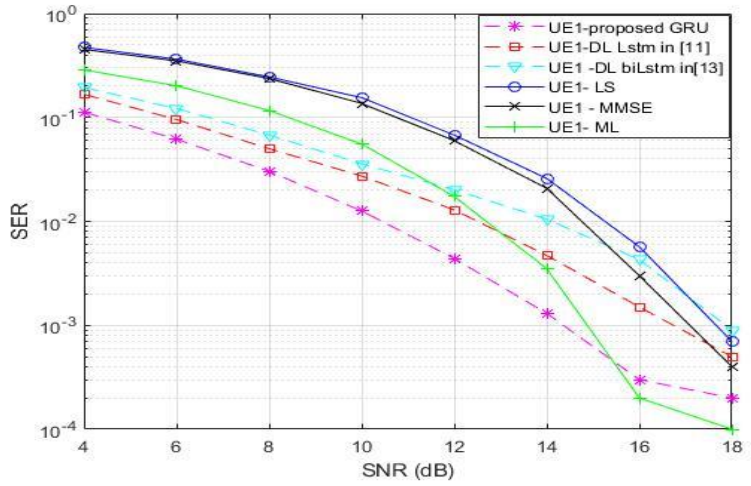


(a)

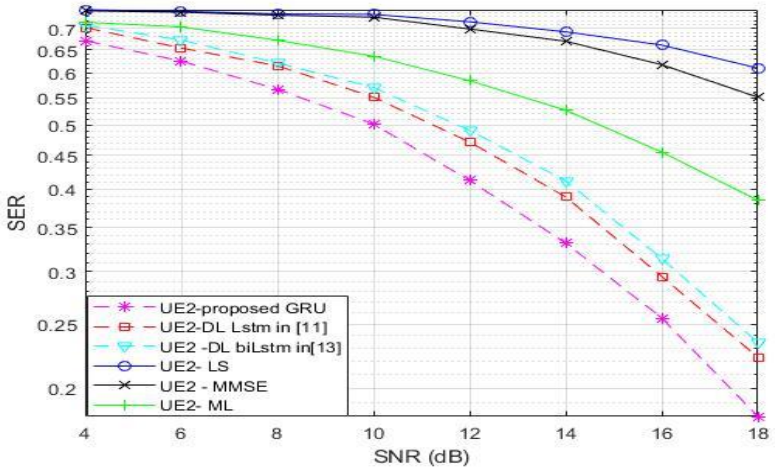


(b)

Figure 4.1 Comparisons between GRU and (pilot- methods , DL systems) at Num of paths is 20, CP is 20 and number of pilots is 64 (a) user1, (b) user2

On the other hand for user1 **the proposed 1-d CNN** outperforms the ML by about 6dB and outperform the proposed GRU by about 4dB.For user2 the proposed 1-d CNN enhancement (the proposed GRU and others DL systems) by about 2dB and ML by about 8dB. Figures (4.2.a, and 4.2.b) show the superiority of the proposed 1-dCNN as compared to pilot-based channel estimation methods and the other DL systems which were mentioned in the literature review. Table (4.4) presents the proposed models alongside existing DL systems in term SER at various SNR values.

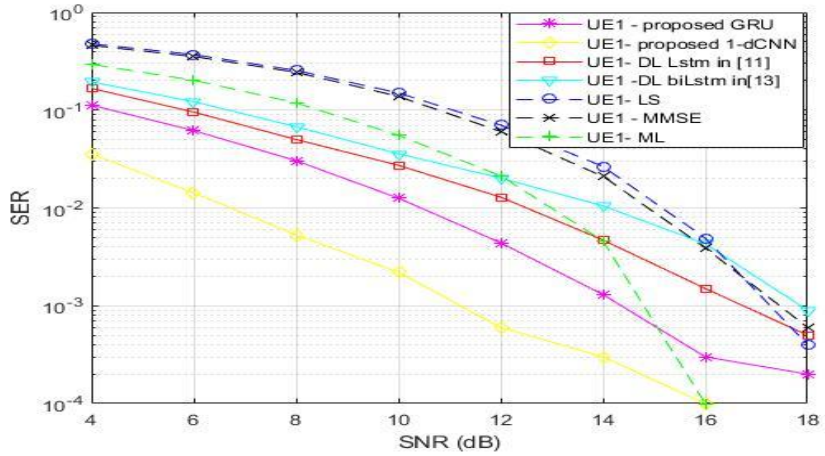


(a)

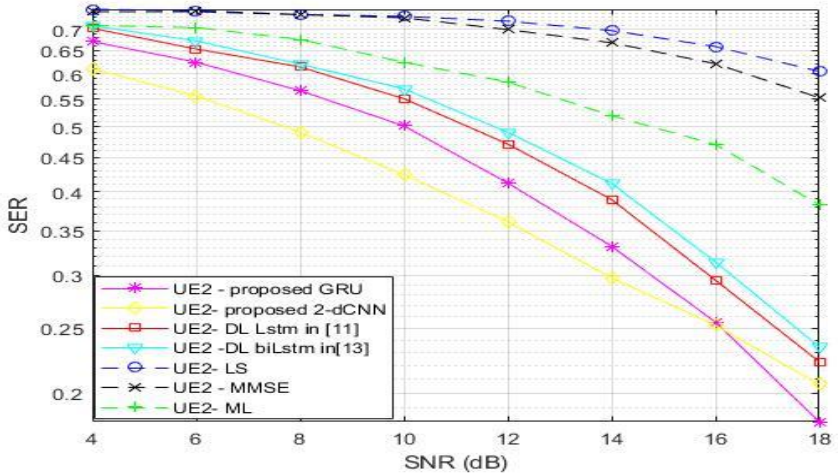


(b)

Figure 4.2 Comparisons between the proposed 1-d CNN and the other DL systems, pilot-based channel estimation methods (a) user1, (b) user2

**Table (4.4) The proposed models alongside existing DL systems when (CP20,Num of paths 20) at various SNR values**

| SNR dB | LSTM [11] SER | | BILSTM [13] SER | | GRU SER | | 1-dCNN SER | |
|---|---|---|---|---|---|---|---|---|
| | User1 | User2 | User1 | User2 | User1 | User2 | User1 | User2 |
| 4 | 0.1672 | 0.7079 | 0.1945 | 0.7078 | **0.1125** | **0.6708** | **0.0355** | **0.6111** |
| 6 | 0.0955 | 0.6539 | 0.122 | 0.6729 | **0.0618** | **0.6249** | **0.0143** | **0.5563** |
| 10 | 0.0273 | 0.4714 | 0.0358 | 0.5701 | **0.0126** | **0.5018** | **0.0022** | **0.4242** |
| 14 | 0.0047 | 0.3894 | 0.0105 | 0.4118 | **0.0013** | **0.3315** | **0.0003** | **0.2976** |
| 18 | 0.0015 | 0.2227 | 0.0043 | 0.2345 | **0.0002** | **0.1812** | **0.0004** | **0.2061** |

## 4.4 Cyclic Prefix Reduction

A cyclic prefix (CP) is often utilized in non-orthogonal multiple access (NOMA) to minimize the wireless system's multipath fading-related inter-symbol interference (ISI). The CP is an image of the transmitted symbol's end that has been included in the symbol's start. The length of the CP must be higher than or equal to the channel length to remove all ISI. If the CP is shorter than the $l$, then the last few symbols of the transmitted sequence will overlap with the beginning of the next symbol due to ISI, which will lead to inter-user interference and degrade the performance of the system.

However, when CP was reduced to 12 the ISI increased, the estimation performance of the MMSE method will degrade and the accuracy of the LS estimate was reduced. ML estimation technique does not depend on the presence or reduction of a cyclic prefix, but the use of a cyclic prefix can improve the performance of the receiver and hence the accuracy of the ML estimation, however it has better performance than LS and MMSE. Deep learning models learn from large amounts of training data, and the presence or absence of a cyclic prefix in the transmitted signals does not directly impact the training process or the resulting learned model.

**The proposed GRU model** outperforms the ML by 4dB for user1 and user2 and it improves [11] by 2dB and [13] by 4db. The performance of [13] significantly deteriorated after reaching 18 dB, closely resembling the performance of the traditional methods. This degradation can be attributed to the occurrence of high vanishing or exploding gradients. These issues in gradient propagation hinder the effective learning and optimization process, leading to diminished performance. Figures (4.3.a, 4.3.b) illustrate the comparisons the proposed GRU model to pilot-based channel estimation methods and the other DL systems.

While **the proposed 1-dCNN** outperforms the ML by about 8dB and outperformance the proposed GRU by about 5dB for user1. Figures (4.3.c , 4.3.d) illustrate the comparisons the proposed 1-dCNN model to pilot-based channel estimation methods and GRU, other DL systems in a literature review when the number of multipath is 20, CP is 12 and number of pilots is 64. Table (4.5) presents the proposed models alongside existing DL systems in term SER at various SNR values.

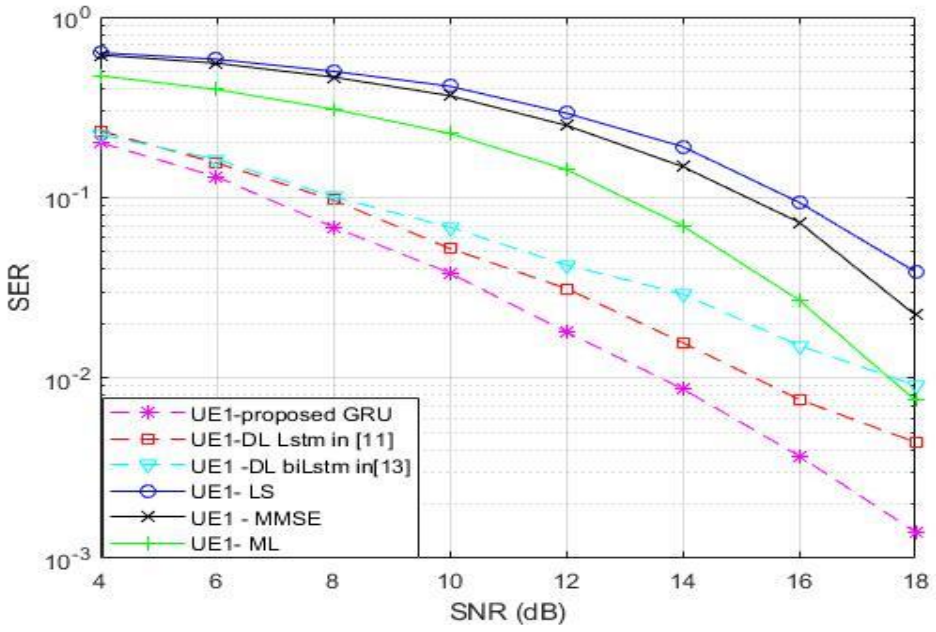


(a)

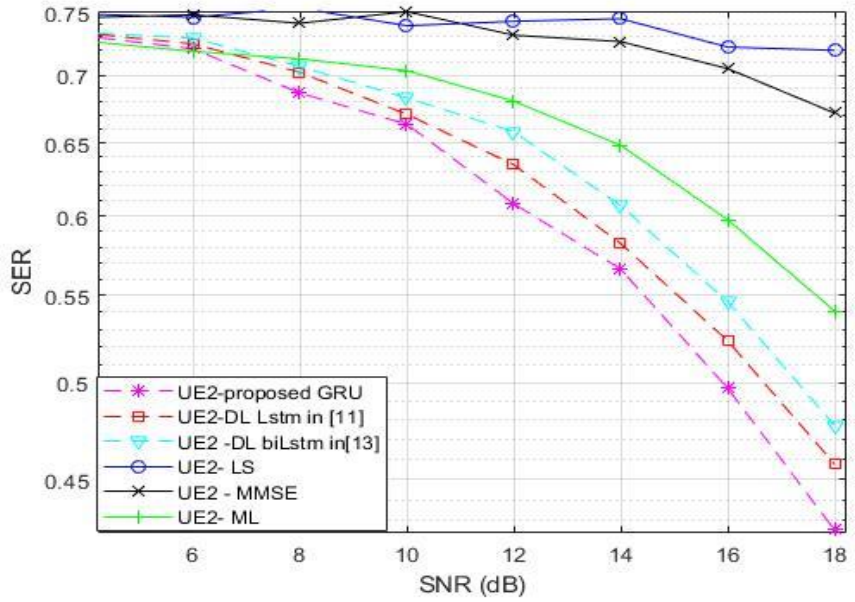
SER
SNR (dB)
UE2-proposed GRU
UE2-DL Lstm in [11]
UE2 -DL biLstm in[13]
UE2- LS
UE2 - MMSE
UE2- ML

(b)

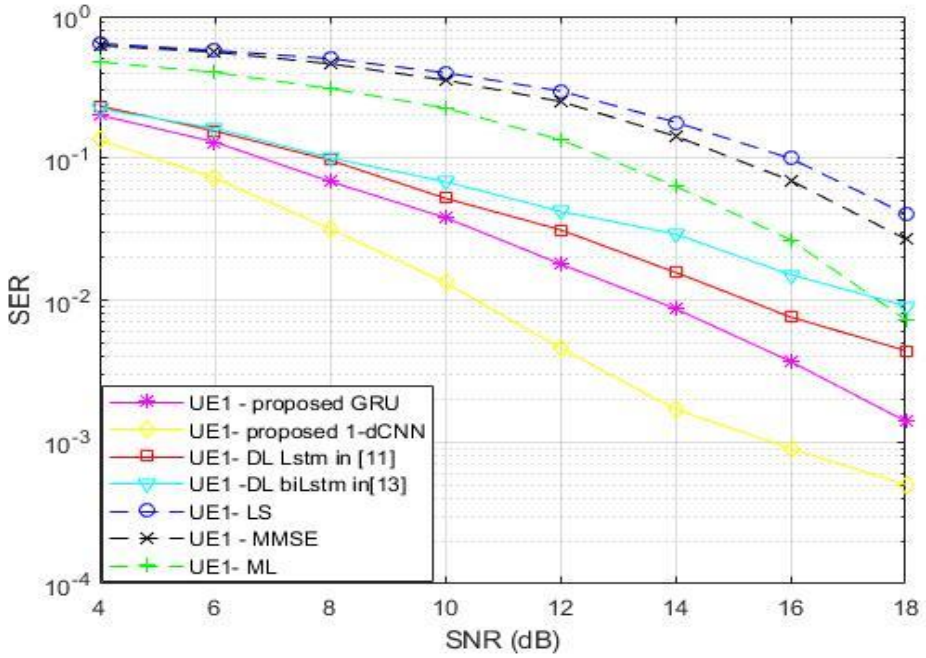
SER
SNR (dB)
UE1 - proposed GRU
UE1- proposed 1-dCNN
UE1- DL Lstm in [11]
UE1 -DL biLstm in[13]
UE1- LS
UE1 - MMSE
UE1- ML

(c)

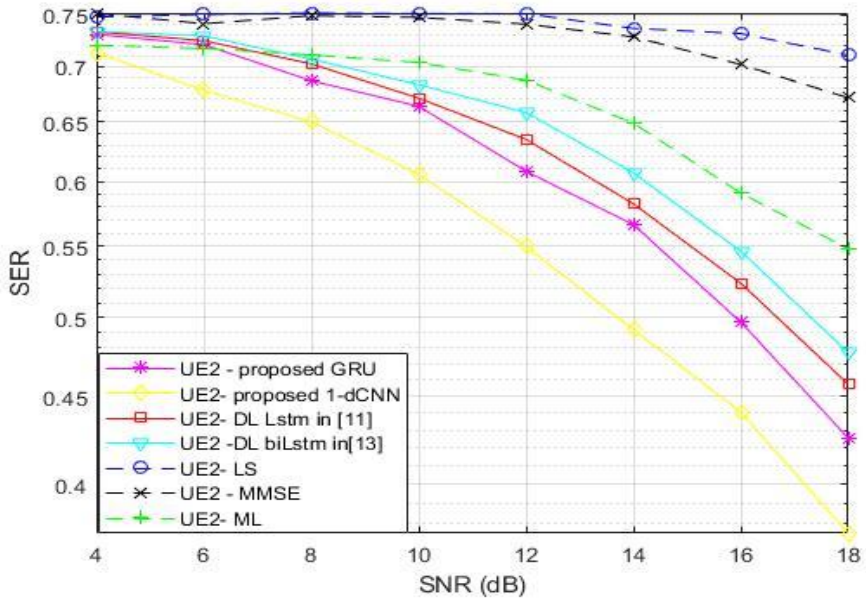


(d)

Figures 4.3 Comparisons between the proposed GRU, 1-d CNN and the other DL systems, pilot-based channel estimation methods with CP 12 (a) user1, (b) user2, (c) user1, (d) user2

**Table (4.5) The proposed models alongside existing DL systems when (CP12,Num of paths 20) at various SNR values**

| SNR dB | LSTM [11] SER | | BILSTM [13] SER | | GRU SER | | 1-dCNN SER | |
|---|---|---|---|---|---|---|---|---|
| | User1 | User2 | User1 | User2 | User1 | User2 | User1 | User2 |
| 4 | 0.2229 | 0.7264 | 0.2229 | 0.7265 | **0.2011** | **0.7263** | **0.1341** | **0.7128** |
| 6 | 0.1088 | 0.7185 | 0.1089 | 0.729 | **0.0686** | **0.7165** | **0.0726** | **0.6778** |
| 10 | 0.0522 | 0.6707 | 0.0684 | 0.6829 | **0.0133** | **0.6635** | **0.0022** | **0.6058** |
| 14 | 0.0157 | 0.5823 | 0.0296 | 0.6069 | **0.0086** | **0.5622** | **0.0017** | **0.4928** |
| 18 | 0.0044 | 0.4574 | 0.0091 | 0.4771 | **0.0014** | **0.4256** | **0.0005** | **0.3747** |

## 4.5 Pilot Reduction

A user will send a symbol of reference known as a "pilot signal" to support receiver channel estimation and signal detection. In NOMA systems, the pilot signal serves as a requirement to discover the user's channel information and accurately allocate resources. However, when the number of a pilot was reduced to 16 the efficacy of MMSE and LS channel estimation methods in NOMA systems may fluctuate depending on the pilot reduction methods used. Reducing the pilot signals can make greater capacity possible for information distribution, but it can also result in less accurate estimates of the channel response. The pilot reduction can also affect ML estimation performance. The DL model can give an acceptable performance with fewer pilot symbols. With user1 **the proposed GRU model** outperforms (ML, [11] and [13]) by 2dB. For user2 the GRU is efficient ML by 4db, [13] by 4dB, and almost symmetrical to [11]. Figures (4.4.a, 4.4.b) illustrate the comparisons the proposed GRU model to pilot-based channel estimation methods and the other DL systems.

On the other hand with user1 **the proposed 1-d CNN** is efficient ML by 6dB, proposed GRU by 5db. For user2 the 1-d CNN is efficient ML by 6db and proposed GRU by 2dB. Figures (4.4.c , 4.4.d) illustrate the comparisons the proposed 1-dCNN model to pilot-based channel estimation methods and GRU, other DL systems. Table (4.6) presents the proposed models alongside existing DL systems in term SER at various SNR values.

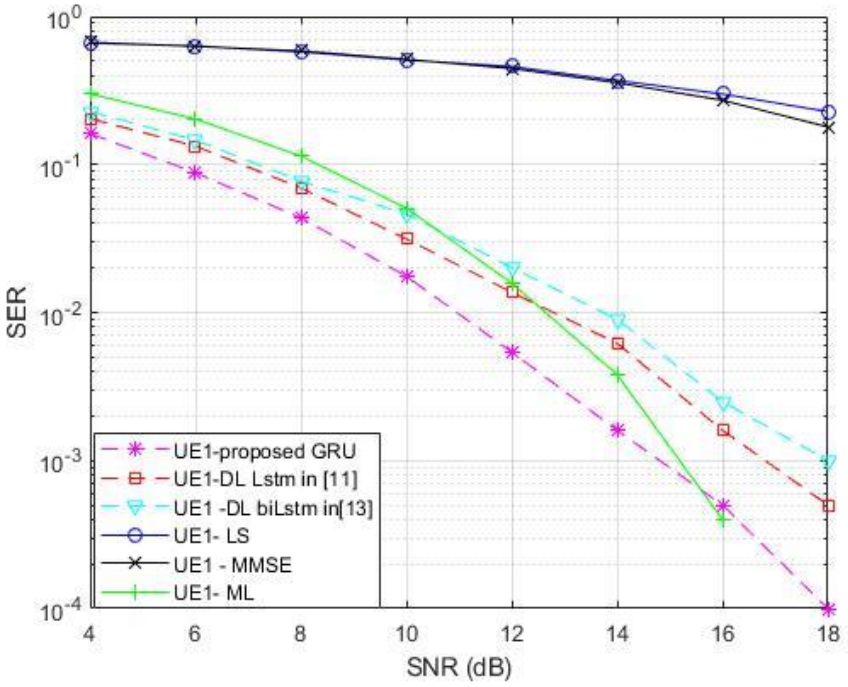
SER
SNR (dB)
UE1-proposed GRU
UE1-DL Lstm in [11]
UE1 -DL biLstm in[13]
UE1- LS
UE1 - MMSE
UE1- ML

(a)

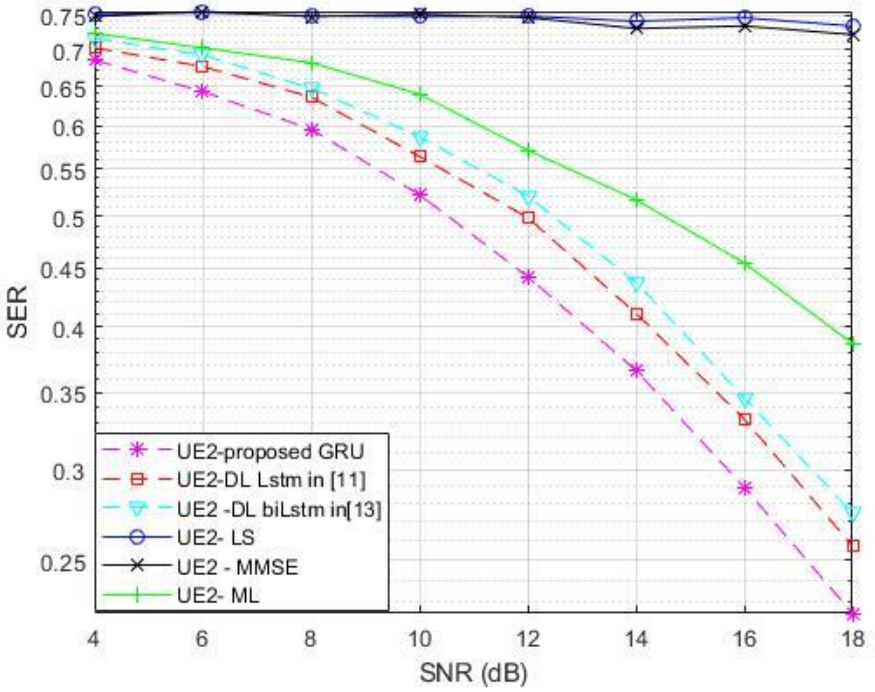
SER
SNR (dB)
UE2-proposed GRU
UE2-DL Lstm in [11]
UE2 -DL biLstm in[13]
UE2- LS
UE2 - MMSE
UE2- ML

(b)

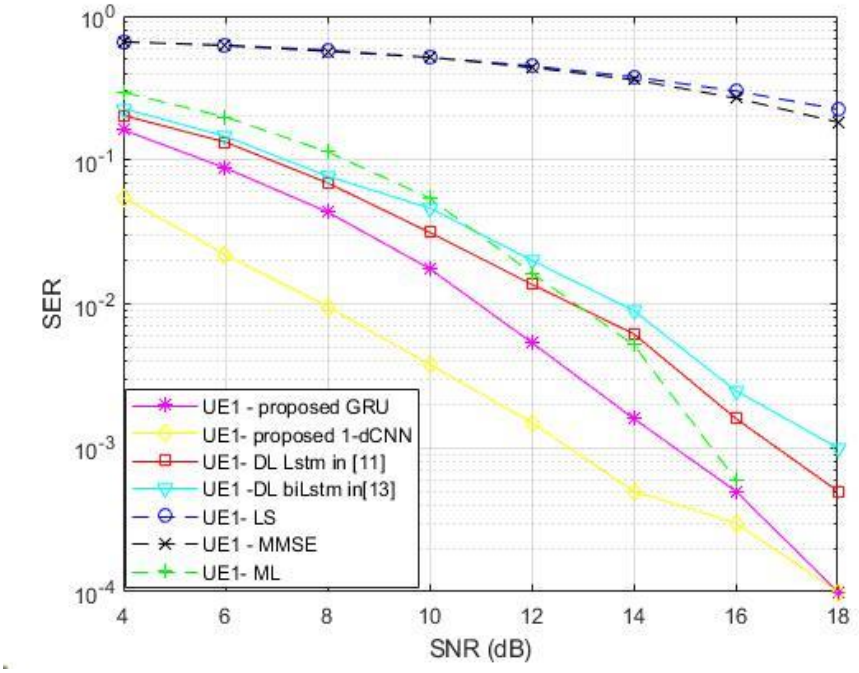


(c)

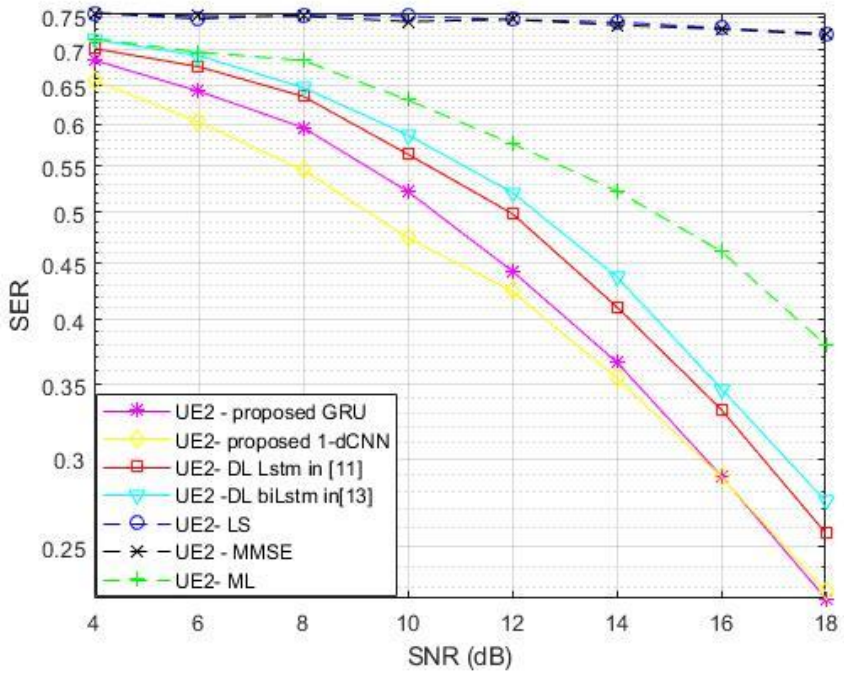


(d)

Figures 4.4 Comparisons between the proposed GRU, 1-dCNN and the others DL systems, pilot-based channel estimation methods with pilot 16 (a) user1, (b) user2, (c) user1, (d) user2

**Table (4.6) The proposed models alongside existing DL systems when (CP 20, Num of pilot 16,Num of paths 20) at various SNR values**

| SNR dB | LSTM [11] SER | | BILSTM [13] SER | | GRU SER | | 1-dCNN SER | |
|---|---|---|---|---|---|---|---|---|
| | User1 | User2 | User1 | User2 | User1 | User2 | User1 | User2 |
| 4 | 0.2039 | 0.702 | 0.2276 | 0.7167 | **0.1616** | **0.6852** | **0.0548** | **0.657** |
| 6 | 0.1331 | 0.676 | 0.146 | 0.6967 | **0.088** | **0.6426** | **0.022** | **0.6028** |
| 10 | 0.0314 | 0.564 | 0.0464 | 0.587 | **0.0176** | **0.5211** | **0.0038** | **0.4742** |
| 14 | 0.0062 | 0.411 | 0.009 | 0.4375 | **0.0016** | **0.3655** | **0.0005** | **0.3545** |
| 18 | 0.0005 | 0.2571 | 0.001 | 0.2747 | **0.0001** | **0.2245** | **0.0001** | **0.2279** |

## 4.6 Number of Multipath

The impact of an increased multipath number in Non-Orthogonal Multiple Access (NOMA) detection and channel estimation can be significant and can affect the performance of the system in several ways especially when in dense environments.In this thesis the assessment is based on the symbol error rate (SER) as a portion of the signal-to-noise ratio (SNR) for different SNR values between 4 dB and 24 dB with a step of 2dB. Multiple paths can result in ISI and inter-user interference, which can make it difficult to identify NOMA signals, and channel estimation, becomes more challenging with a high fading where accurate channel estimation is essential for the proper detection of NOMA signals. With this number of multipath, pilot-based channel estimation methods become more complex, and the accuracy of the estimation will decrease. However DL systems better performance than pilot-based channel estimation methods, this methods field to detect signal and error rate is very high. However, when we increased the number of multipath to 30 and CP to 30 and tested the proposed models, we have obtained good results in this field.

For user1 **the proposed GRU** showed a relatively simple superiority over other deep learning systems until 14db, Performance seemed to degrade. In contrast

**the proposed 1-dCNN** outperforms the proposed GRU and the other DL systems for (U1 and U2). Figure (4.5.a, 4.5.b,) show the comparisons between the proposed GRU, 1-d CNN and the pilot-based channel estimation methods and the other DL systems in a literature review when the number of multipath is 30, CP is 30 and number of pilots is 64.

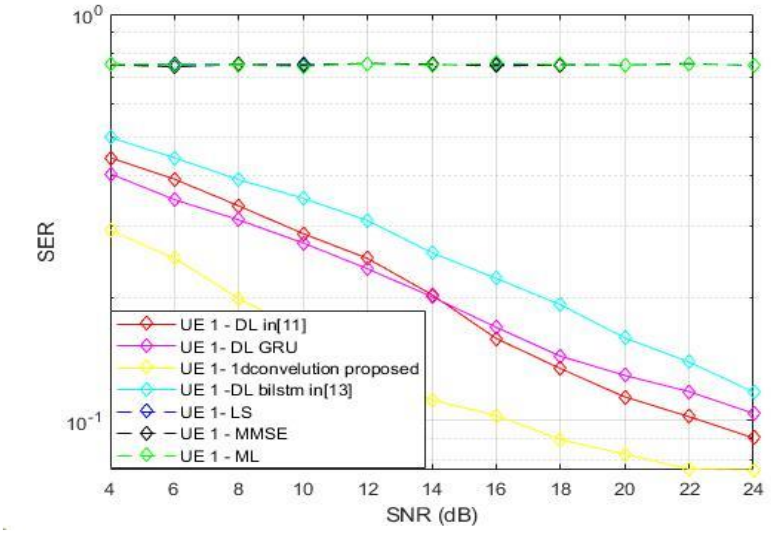


(a)

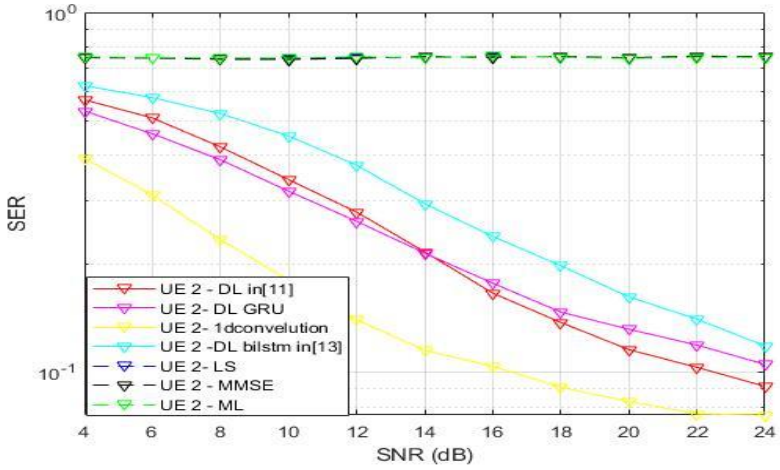


(b)

Figure 4.5 SNR / SER Number of multipath is 30, CP is 30 and number of pilots is 64 (a) user1, (b) user

**Table (4.7) Comparison table at 14 dB SNR**

| No | Reference | DL-type | SER per subcarrier when pilot 64, CP20,path 20 | | SER per subcarrier when pilot64, CP12,path 20 | | SER per subcarrier when pilot16, CP20,path 20 | |
|---|---|---|---|---|---|---|---|---|
| | | | User1 | User2 | User1 | User2 | User1 | User2 |
| 1 | J. Thompson, 2019,[10] | LSTM | 0.05 | 0.8 | 0.75 | 0.8 | 0.55 | 0.84 |
| 2 | A. Hilal, 2022, [11]. | LSTM | 0.003 | 0.36 | 0.015 | 0.58 | 0.005 | 0.4 |
| 3 | D.V. Rahman, 2022, [13]. | BILSTM | 0.009 | 0.4 | 0.03 | 0.62 | 0.009 | 0.45 |
| 4 | A.H.Ali, 2022,[21] | LSTM+ CNN | **$10^{-10}$** | **0.20** | 0.02 | 0.55 | - | - |
| 5 | **Proposed 1 (GRU)** | GRU | 0.001 | 0.35 | 0.009 | 0.53 | 0.002 | 0.3718 |
| 6 | **Proposed 2 (1-dCNN)** | 1-dCNN | 0.0002 | 0.24 | **0.002** | **0.5** | **0.0002** | **0.34** |

## 4.7 Network Training Time

Training time is crucial in deep learning because it affects the overall development time, cost, and iteration speed. Shorter training times enable faster experimentation and development, allowing for quicker improvements and better results. However, when we used a computer that has specifications, processor Intel® core i5-7210M CPU@ 2.50GHZ, 2cores, external graphics card NVidia GeForce 630*2GB. The proposed models demonstrate shorter training times compared to other deep learning systems mentioned in the literature review. Table 4.8 illustrates this observation. Specifically, the GRU model requires 24 minutes, while the 1-d CNN model needs 20 minutes for training. Despite the shorter training times, both models exhibit high performance. This suggests that these two systems are effective and promising deep learning models.

**Table (4.8) Time training for different deep neural networks**

| Refrerences | Time in minute |
|---|---|
| The proposed joint detector based GRU system | 24 |
| **The proposed joint detector based 1-d CNN system** | **20** |
| J. Thompson et al ,2019, [10] | 90 |
| A. Hilal, 2022, [11]. | 28 |
| D.V. Rahman et al,2022, [13] | 35 |

## 4.8 Training Accuracy and Validation Accuracy

The proposed models showcases impressive generalization in relation to training and validation accuracy, surpassing alternative deep learning systems mentioned in the literature review that were designed to counter overfitting with strong generalization. Notably, the proposed model exhibits superior performance. This comparison is visually depicted in Table (4.9)

**Table (4.9) Comparison of training accuracy and validation accuracy for different DL models**

| Reference | DL-type | DNN structure | No.of CNN Layers | No.of filters | Filter size | Training accuracy (%) | Validation accuracy (%) |
|---|---|---|---|---|---|---|---|
| A. Hilal, 2022, [11]. | LSTM | 64 LSTM Unit | ------ | ------ | ------- | 90.28 | 74.8 |
| R.S.H. AL-Musawi,2022,[20] | CNN | -------- | 3 | 32 | (7,7) | 61.11 | 60.10 |
| A.H.Ali, 2022,[21] | LSTM + CNN | 64 LSTM Unit | 1 | 32 | (5,5) | 88.61 | 85.36 |
| **Proposed 1 (GRU)** | GRU | 64 GRU Unit | ------- | ------- | ------- | **95.9607** | **95.7** |
| **Proposed 2 (1-dCNN)** | 1-dCNN | --------- | 2 | 32 | 3 | **92.1424** | **92.1403** |

# CHAPTER FIVE
# Conclusion and Future Works

# CHAPTER FIVE
# Conclusion and Future Works

## 5.1 Conclusions

The primary objective of this thesis aimed to enhance (NOMA) efficiency by utilizing deep learning (DL) techniques for joint signal detection and channel estimation. The study aimed to propose and evaluate two new DL approaches while considering different system parameters and operating conditions. The performance assessment of the proposed DL approaches for enhancing statical NOMA systems are based on the SER as an expression of SNR. The SNR is varied between 4 dB and 18dB with a step size of 2dB.

**The first proposed approach:-**

- The thesis introduces a one-shot deep learning system based on the gate recurrent units (GRU) architecture. This architecture differs from conventional (LSTM) networks in that it only has two gates (update and reset). The GRU-based method provides better performance and stability in deep learning tasks by minimizing time dependence and successfully addressing the difficulties caused by vanishing or expanding gradients in recurrent neural networks (RNNs).
- The extensively tested GRU-based technique, specifically with GRU layer=64, delivers promising results, getting a training accuracy of 95.9607% and a validation accuracy of 95.7%. Its impressive generalization potential and low overfitting highlight its capacity to effectively learn from training data without memorization.
- In terms (SNR), the proposed GRU-based approach performs 2dB better than the LSTM in [11] and 4dB better than the BILSTM in [13]. Additionally, it keeps its outstanding results even when low (SNR) and

significant parameters like the number of pilots and the (CP) are decreased while raising the number of paths ($l$).

- In this work, conventional techniques such as ML, MMSE, and LS were examined. The proposed model outperformed LS, with MMSE performing better than LS. ML presents the best performance among the three techniques. Notably, in the perfect case scenario (($l$) = CP), and at 16dB, the proposed model demonstrated similar performance to ML, indicating its competitive accuracy and reliability. However, the effectiveness of these conventional techniques decreased significantly when the CP and the number of pilots were reduced.
- The proposed approach exhibits efficiency in terms of training duration, completing the training process in approximately 24 minutes. This training time is 4 minutes faster than the approach in [11] and 11 minutes faster than the approach in [13].

**The second proposed approach:-**

- The thesis presents a1-d CNN architecture capable of extracting and classifying features independently of time dependencies. It utilizes two sets of 1-d Conv-Layers with a filter weight =32, filter size =3, and a stride=2. The training accuracy achieved is 92.1424%, with a validation accuracy of 92.1403%. The close match between the training and validation accuracies indicates successful learning without overfitting.
- The 1-dCNN outperforms the state-of-the-art approaches [11, 13] and conventional techniques in the ideal case scenario. It also outperforms the proposed GRU-based approach by 4dB. Notably, the performance remains strong even with reduced system parameters such as low (SNR), reduced CP, and a lower number of pilots. Specifically, the 1D CNN outperforms the GRU-based approach by 3dB when the CP is reduced and by 4dB when the number of pilots is reduced.

- When the $(l)$ reaches 30 and the CP are set to 30, the performance of conventional methods deteriorates significantly. In contrast, suggested 1d CNN outperforms the proposed GRU and the approach in [11] by 6dB, as well as the approach in [13] by 8dB. These findings demonstrated that the suggested 1-dCNN exhibits robustness in dense environments and performs exceptionally well under challenging conditions.
- 1-d CNN-based DL system trains approximately 4 minutes faster than the GRU-based system.

## 5.2 Future works

In order to further enhance the performance of Deep Learning-based approaches for NOMA systems, several avenues of future work can be explored. In this section, discuss some potential areas of research that can be pursued in order to improve the robustness and efficiency of DL techniques for joint signal detection and channel estimation in NOMA systems. These suggestions can serve as a starting point for researchers who are interested in further developing DL-based NOMA systems.

1. Developing adaptive deep learning algorithms that can adjust their parameters and structure dynamically based on the channel conditions, to achieve better performance and flexibility.
2. Evaluating the performance of deep learning-based NOMA systems in practical environments with interference and mobility, and proposing solutions to mitigate their impact on the performance of the system.
3. Investigating the potential of combining deep learning-based signal detection and channel estimation with other advanced techniques, such as beamforming and massive MIMO, to further improve the spectral efficiency and reliability of NOMA-OFDM systems.

4. Investigating the effectiveness of other types of deep learning models, such as Transformer-based architectures, for signal detection and channel estimation in NOMA-OFDM systems.

# References

[1] Z. Ding and H. V. Poor, "Advantages of NOMA for Multi-User BackCom Networks," *in IEEE Communications Letters,* vol. 25, no. 10, pp. 3408-3412, Oct. 2021.

[2] S. M. Islam, M. Zeng, and O. A. Dobre, "NOMA in 5G systems: Exciting possibilities for enhancing spectral efficiency," *arXiv preprint arXiv: 1706.08215,* vol.1, no.2, Jun. 2017.

[3] M. K. Hasan, M. Shahjalal, M. M. Islam, M. M. Alam, M. F. Ahmed and Y. M. Jang, "The Role of Deep Learning in NOMA for 5G and Beyond Communications," *2020 International Conference on Artificial Intelligence in Information and Communication (ICAIIC),* Fukuoka, Japan, pp. 303-307, Feb . 2020.

[4] H. S. Ghazi and K. W. Wesołowski, "Improved Detection in Successive Interference Cancellation NOMA OFDM Receiver," *in IEEE Access,* vol. 7, pp. 103325-103335, Jul.2019.

[5] M. R. Usman, A. Khan, M. A. Usman, Y. S. Jang and S. Y. Shin, "On the performance of perfect and imperfect SIC in downlink non orthogonal multiple access (NOMA)," *2016 International Conference on Smart Green Technology in Electrical and Information Systems (ICSGTEIS),* Denpasar, Indonesia, Oct.2016, pp. 102-106.

[6] V. Andiappan and V. Ponnusamy, "Deep learning enhanced NOMA system: A survey on future scope and challenges," *Wireless Pers Commun 123*, pp. 839–877, Mar.2022.

[7] H. Ye, L. Liang, G. Y. Li and B. -H. Juang, "Deep Learning-Based End-to-End Wireless Communication Systems With Conditional GANs as Unknown Channels," *in IEEE Transactions on Wireless Communications*, vol. 19, no. 5, pp. 3133-3143, May. 2020.

[8] A. L. Ha, T. Van Chien, T. H. Nguyen, W. Choi and V. D. Nguyen, "Deep Learning-Aided 5G Channel Estimation," *2021 15th International Conference on Ubiquitous Information Management and Communication (IMCOM),* Seoul, Korea (South), Jan.2021, pp. 1-7.

[9] S. A. H. Mohsan, Y. Li, A. V. Shvetsov, J. Varela-Aldás, S. M. Mostafa, and A. Elfikky, "A Survey of Deep Learning Based NOMA: State of the Art, Key Aspects, Open Challenges and Future Trends," *Sensors,* vol. 23, no. 6, p. 2946, Mar. 2023.

[10] Narengerile and J. Thompson, "Deep Learning for Signal Detection in Non-Orthogonal Multiple Access Wireless Systems," *2019 UK/ China Emerging Technologies (UCET),* Glasgow, UK, Sep.2019, pp. 1-4.

[11] A. H. Ali, R. S. A. Musawi, and K. A. Majdi, "Enhancements to the Deep Learning Signal Detection Model in Non-Orthogonal Multiple

Access Receivers and Noisy Channels," *Journal of telecommunications and the Digital Economy*, Vol. 10, No. 1, pp. 92-100, Mar.2022.

[12] S. Pandya, M.A. Wakchaure , R. Shankar and J.R Annam, "Analysis of NOMA-OFDM 5G wireless system using deep neural network," *The Journal of Defense Modeling and Simulation*,Vol.19,No.4, pp.799-806, Oct.2022.

[13] D.V.Rahman, M. Habibur, M. A. S. Sejan, S. G. Yoo, M.A. Kim, Y.H. You, and H.K.Song, "Multi-User Joint Detection Using Bi-Directional Deep Neural Network Framework in NOMA-OFDM System," *Sensors*, Vol. 22, No. 18, pp.6994, 2022.

[14] A. Bhatt ,R. Shankar, G. Niedbala and A. Rupani, "Analysis of the Fifth Generation NOMA System using LSTM Algorithm," *International Journal of Computing and Digital Systems*,vol.11,no.1, pp.215-223, Feb 2022.

[15] M. A. Aref and S. K. Jayaweera, "Deep Learning-aided Successive Interference Cancellation for MIMO-NOMA," *GLOBECOM 2020 - 2020 IEEE Global Communications Conference*, Taipei, Taiwan, 2020, pp.1-5.

[16] A. L. Ha, T. Van Chien, T. H. Nguyen, W. Choi and V. D. Nguyen, "Deep Learning-Aided 5G Channel Estimation," *2021 15th International Conference on Ubiquitous Information Management and Communication (IMCOM)*, Seoul, Korea (South), 2021, pp. 1-7.

[17] S.Isaac, Y. G.Sun, D.Lee, S. H. Kim, J. Lee, J.H. Kim, Y.Shin and J.Y. Kim, "Deep learning based successive interference cancellation scheme in no orthogonal multiple access downlink network," *Energies* ,Vol.13, no. 23, pp. 6237, 2020.

[18] Y. Xie, K. C. Teh, and A. C. Kot, "Deep learning-based joint detection for OFDM-NOMA scheme," *IEEE Communications Letters*, Vol. 25, No. 8, pp. 2609-2613, 2021.

[19] K. Dharmesh, P. Trada, H. Kaswala and H. B. Shah, "DEEP LEARNING BASED SIGNAL DETECTION AND CHANNEL ESTIMATION FOR MIMO-NOMA SYSTEM," *Science*, Vol .01, No. 01, pp. 23-35, 2022.

[20] R.S.AL-Musawi, A. H.Ali, K.Al-Majdi and S. Al Gayar, "Development of a convolutional neural network joint detector for non-orthogonal multiple access uplink receivers," *EUREKA: Physics and Engineering*, No.4, pp.170, 2022.

[21] A. H. Ali, R. S. A. Musawi, and K. A. Majdi, "Development of CNN-LSTM Hybrid Deep Learning Network for the Joint Detection of Non-Orthogonal Multiple Access Signals in 5G Uplink Receivers," *International Journal of Intelligent Engineering and Systems*, Vol.15, No.4, May. 2022.

[22] K. Selvam and K. Kumar, "Energy and Spectrum Efficiency Trade-off of Non-Orthogonal Multiple Access (NOMA) over OFDMA for Machine-to-Machine Communication," *2019 Fifth International Conference on Science Technology Engineering and Mathematics (ICONSTEM)*, Chennai, India, 2019, pp. 523-528.

[23] A. Khalili and D. W. K. Ng, "Energy and Spectral Efficiency Tradeoff in OFDMA Networks via Antenna Selection Strategy, " *2020 IEEE Wireless Communications and Networking Conference (WCNC), Seoul*, Korea (South), 2020, pp. 1-6.

[24] Z. Ding, X. Lei, G. K. Karagiannidis, R. Schober, J. Yuan and V. K. Bhargava, "A Survey on Non-Orthogonal Multiple Access for 5G Networks: Research Challenges and Future Trends, " in *IEEE Journal on Selected Areas in Communications*, vol. 35, no. 10, pp. 2181-2195, Oct. 2017.

[25] Z. Yang, Z. Ding, P. Fan and N. Al-Dhahir, "The Impact of Power Allocation on Cooperative Non-orthogonal Multiple Access Networks With SWIPT, " in *IEEE Transactions on Wireless Communications*, vol. 16, no. 7, pp. 4332-4343, Jul. 2017.

[26] Z. Ding, R. Schober and H. V. Poor, "Unveiling the Importance of SIC in NOMA Systems—Part 1: State of the Art and Recent Findings, " in *IEEE Communications Letters*, vol. 24, no. 11, pp. 2373-2377, Nov. 2020.

[27] Z. Ding, R. Schober and H. V. Poor, "Unveiling the Importance of SIC in NOMA Systems—Part II: New Results and Future Directions, " in *IEEE Communications Letters*, vol. 24, no. 11, pp. 2378-2382, Nov. 2020.

[28] S. Guo and X. Zhou, "Robust Resource Allocation With Imperfect Channel Estimation in NOMA-Based Heterogeneous Vehicular Networks, " in *IEEE Transactions on Communications*, vol. 67, no. 3, pp. 2321-2332, Mar. 2019.

[29] T. Kebede, Y. Wondie, J. Steinbrunn, H. B. Kassa and K. T. Kornegay, "Multi-Carrier Waveforms and Multiple Access Strategies in Wireless Networks: Performance, Applications, and Challenges," in *IEEE Access*, vol. 10, pp. 21120-21140, Feb. 2022.

[30] S.Rupesh, "Multiple access techniques for 4G mobile wireless networks," *International Journal of Engineering Research and Development*, vol. 5, no.11, pp.86-94, Feb. 2013.

[31] Z.Wei, J.Yuan, D. W. K. Ng, M. Elkashlan and Z. Ding, "A survey of downlink non-orthogonal multiple access for 5G wireless communication networks, " *arXiv preprint arXiv: 1609.01856*, Sep.2016.

[32] M. Aldababsa, M. Toka, S. Gökçeli, G. K. Kurt and O. Kucur, "A tutorial on non-orthogonal multiple access for 5G and beyond," *Wireless communications and mobile computing*, Jun.2018.

[33] L. Dai, B. Wang, Y. Yuan, S. Han, I. Chih-lin and Z. Wang, "Non-orthogonal multiple access for 5G: solutions, challenges, opportunities, and future research trends, " in *IEEE Communications Magazine*, vol. 53, no. 9, pp. 74-81, Sep. 2015.

[34] A. Li, Y. Lan, X. Chen and H. Jiang, "Non-orthogonal multiple access (NOMA) for future downlink radio access of 5G," in *China Communications*, vol. 12, no. Supplement, pp. 28-37, Dec. 2015.

[35] N. Iswarya, L.S. Jayashree, "A survey on successive interference cancellation schemes in non-orthogonal multiple access for future radio access," *Wireless Personal Communications*, vol. 120, no.2, pp.1057-1078, Sep.2021.

[36] Y. Saito, Y. Kishiyama, A. Benjebbour, T. Nakamura, A. Li and K. Higuchi, "Non-Orthogonal Multiple Access (NOMA) for Cellular Future Radio Access," *2013 IEEE 77th Vehicular Technology Conference (VTC Spring)*, Dresden, Germany, 2013, pp. 1-5.

[37] W. U. Khan, F. Jameel, T. Ristaniemi, B. M. Elhalawany and J. Liu, "Efficient Power Allocation for Multi-Cell Uplink NOMA Network," *2019 IEEE 89th Vehicular Technology Conference (VTC2019-Spring)*, Kuala Lumpur, Malaysia, 2019, pp. 1-5.

[38] Y. Liu, Z. Ding, M. Elkashlan and J. Yuan, "Nonorthogonal Multiple Access in Large-Scale Underlay Cognitive Radio Networks, " in *IEEE Transactions on Vehicular Technology*, vol. 65, no. 12, pp. 10152-10157, Dec. 2016.

[39] Y. Liu, Z. Qin, M. Elkashlan, Z. Ding, A. Nallanathan and L. Hanzo, "Nonorthogonal Multiple Access for 5G and Beyond, " in *Proceedings of the IEEE*, vol. 105, no. 12, pp. 2347-2381, Dec. 2017.

[40] Y. Saito, Y. Kishiyama, A. Benjebbour, T. Nakamura, A. Li and K. Higuchi, "Non-Orthogonal Multiple Access (NOMA) for Cellular Future Radio Access," *2013 IEEE 77th Vehicular Technology Conference (VTC Spring)*, Dresden, Germany, 2013, pp. 1-5.

[41] P. Sharma, A. Kumar and M. Bansal, "Performance Analysis of P-N-NOMA Over Generalized Fading Channel," in *IEEE Access*, vol. 8, pp. 105962-105971, 2020.

[42] S. M. Islam, M.Zeng, O.A.Dobre and K. S. Kwak, "Non-orthogonal multiple access (NOMA): How it meets 5G and beyond," *arXiv preprint arXiv: 1907.10001*. Jul .2019.

[43] K. Saito, A. Benjebbour, Y. Kishiyama, Y. Okumura and T. Nakamura, "Performance and design of SIC receiver for downlink NOMA with open-loop SU-MIMO, " *2015 IEEE International Conference on Communication Workshop (ICCW)*, London, UK, 2015, pp. 1161-1165.

[44] Z. Ding, R. Schober, P. Fan and H. Vincent Poor, " OTFS-NOMA: An Efficient Approach for Exploiting Heterogenous User Mobility Profiles, " in *IEEE Transactions on Communications*, vol. 67, no. 11, pp. 7950-7965, Nov. 2019.

[45] Z. Yang, W. Xu, C. Pan, Y. Pan and M. Chen, "On the Optimality of Power Allocation for NOMA Downlinks With Individual QoS Constraints, " *in IEEE Communications Letters*, vol. 21, no. 7, pp. 1649-1652, July. 2017.

[46] F. Kara and H. Kaya, "BER performances of downlink and uplink NOMA in the presence of SIC errors over fading channels," *IET Communications*, vol.12, no. 15, pp.1834-1844, Sep.2018.

[47] Chen, Xinyi, Huarui Yin, and Guo Wei. "Impact of frequency offset on the performance of uplink OFDM-NOMA systems." 2018 IEEE 4th International Conference on Computer and Communications (ICCC). IEEE, 2018.

[48] M. F. Kader, M. B. Shahab and S. Y. Shin, "Exploiting Non-Orthogonal Multiple Access in Cooperative Relay Sharing," in *IEEE Communications Letters*, vol. 21, no. 5, pp. 1159-1162, May .2017.

[49] Cho, Yong Soo, Jaekwon Kim, Won Y. Yang, and Chung G. Kang. MIMO-OFDM wireless communications with MATLAB. John Wiley & Sons, 2010.

[50] B.Souleymane, S.R.Mondol and Z.Wei, "Comparative Performance Study of LS and MMSE Channel Estimation over Time Varying Channel in OFDM System," *International Journal of Engineering Research*, vol.5, no. 03, Mar.2016.

[51] M. H.Hsieh and C. H. Wei, "Channel estimation for OFDM systems based on comb-type pilot arrangement in frequency selective fading channels," *IEEE Transactions on Consumer Electronics*, vol.44, no. 1, pp.217-225, Feb.1998.

[52] Goldsmith, Andrea. Wireless communications. Cambridge university press, 2005.

[53] H. Ye, G. Y. Li and B. -H. Juang, "Power of Deep Learning for Channel Estimation and Signal Detection in OFDM Systems, " in *IEEE Wireless Communications Letters*, vol. 7, no. 1, pp. 114-117, Feb. 2018.

[54] I.Goodfellow, Y. Bengio, and A. Courville, Deep Learning. MIT press, Cambridge, Massachusetts, M.A.2016.

[55] N.Khare, P.Devan, C. L.Chowdhary, S.Bhattacharya, G.Singh, S.Singh and B.Yoon, (2020), "Smo-dnn: Spider monkey optimization and deep neural network hybrid classifier model for intrusion detection," *Electronics*, vol.9, no.4, pp.692, Apr.2020.

[56] K.Smagulova, and A. P. James, "Overview of long short-term memory neural networks," Deep Learning Classifiers with Memristive Networks: Theory and Applications, pp. 139-153, 2020.

[57] U. Michelucci, "Applied Deep Learning," A Case-Based Approach to Understanding Deep Neural Networks, 2018.

[58] J. Jin, C. Zhang, F. Feng, W. Na, J. Ma and Q. -J. Zhang, "Deep Neural Network Technique for High-Dimensional Microwave Modeling and Applications to Parameter Extraction of Microwave Filters, " in *IEEE Transactions on Microwave Theory and Techniques*, vol. 67, no. 10, pp. 4140-4155, Oct. 2019.

[59] G. Shen, Q. Tan, H. Zhang, P .Zeng and J .Xu, "Deep learning with gated recurrent unit networks for financial sequence predictions," *Procedia computer science*, Vol. 131,pp.895-903, Jan.2018.

[60] M. Ravanelli, P .Brakel, M. Omologo and Y .Bengio, "Light gated recurrent units for speech recognition," *IEEE Transactions on Emerging Topics in Computational Intelligence*,Vol.2 , No. 2, pp.92-102,Mar. 2018.

[61] S.Kiranyaz, O.Avci, O.Abdeljaber, T.Ince, M.Gabbouj and D. J. Inman, "1D convolutional neural networks and applications: A survey," *Mechanical systems and signal processing*, vol.151, pp.107398, Apr.2021.

[62] T.Liu, H.Xu, M.Ragulskis, M.Cao and W.Ostachowicz, "A data-driven damage identification framework based on transmissibility function datasets and one-dimensional convolutional neural networks: Verification on a structural health monitoring benchmark structure," *Sensors*, vol.20, no.4, pp.1059, Feb.2020.

[63] M.Pérez-Enciso and L. M. Zingaretti, "A guide on deep learning for complex trait genomic prediction," *Genes*, vol.10, no.7, pp.553, Jul.2019.

[64] A.Krizhevsky, I.Sutskever, and G. E. Hinton, "Imagenet classification with deep convolutional neural networks," *Communications of the ACM*, vol. 60, no. 6, pp.84-90, May.2017.

[65] M.Lin, Q.Chen, and S.Yan, "Network in network," *arXiv preprint arXiv: 1312.4400*, Dec.2013.

[66] Z. Li, F. Liu, W. Yang, S. Peng and J. Zhou, "A Survey of Convolutional Neural Networks: Analysis, Applications, and Prospects," in *IEEE*

*Transactions on Neural Networks and Learning Systems*, vol. 33, no. 12, pp. 6999-7019, Dec. 2022.

[67] J. Xu, Z. Li, B. Du, M. Zhang and J. Liu, "Reluplex made more practical: Leaky ReLU," *2020 IEEE Symposium on Computers and Communications (ISCC)*, Rennes, France, 2020, pp. 1-7.

[68] X.Fan, W.Jiang, H.Luo and M.Fei, (2019). "Spherereid: Deep hypersphere manifold embedding for person re-identification," *Journal of Visual Communication and Image Representation*, vol.60, pp.51-58, Apr.2019.

[69] B.Gao and L. Pavel, "On the properties of the softmax function with application in game theory and reinforcement learning," arXiv *preprint arXiv: 1704.00805*.Apr.2017.

**الخلاصة :**

يسعى الجيل القادم من الاتصالات اللاسلكية إلى التفوق على الوصول المتعدد المتعامد (**OMA**) من حيث الكفاءة ودعم المستخدمين. فهي توفر كفاءة طيفية محسنة وتقليل في التأخير، ولكن قد تتأثر كفاءتها في حالة وجود كشف إشارة غير مثالي. يتألق الوصول المتعدد غير المتعامد (**NOMA**) في هذا الصدد، مما يسمح للعديد من المستخدمين والخدمات بالوصول إلى جميع الموجات الحاملة الفرعية دون قيود التعامد. ومع ذلك، مع زيادة عدد المستخدمين يمكن أن يعيق كفاءة استخدام الطاقة. يوفر النظام الهجين (**OFDM-NOMA**) نهجًا قويًا لمواجهة هذه التحديات وتحسين الكفاءة الطيفية بشكل كبير، حيث ينقل حزم مستخدمين المتعددة كإشارة واحدة، مما يتطلب خوارزميات استقبال متقدمة مثل إلغاء التداخل المتتالي (**SIC**). تتطلب الانظمة المعتمدة على SIC تتبعًا مثاليًا لحالة القناة من خلال بعض تقنيات تقديرتاثيرالقناة.عندما يكون تقدير القناة غير مثالي ، سوف يؤثر على موثوقية **SIC**.

ولمواجهة هذا التحدي بشكل فعال، هناك طريقة مثيرة تتضمن تسخير قدرات خوارزميات التعلم العميق (**DL**) للكشف السريع عن الإشارة وتقدير القناة في سيناريوهات المحاولة الواحدة. تقترح هذه الرسالة طريقتين جديدتين للتعلم العميق لتحسين الكشف الهجين عن اشارة(**OFDM-NOMA**). **النهج الاول** هو خوارزمية بوابات الوحدات المتكررة (**GRU**). تحتوي GRU على بوابتين (التحديث وإعادة التعيين)، مما يعمل على تحسين الأداء من خلال تقليل الاعتماد على الوقت ومعالجة التدرجات في الشبكات العصبية المتكررة (RNN).

**النهج الثاني** المقترح هو الشبكات العصبية التلافيفية أحادية الابعاد(1-dCNN). يعالج هذا النهج القيود المفروضة على أساليب **DL** الحالية باستخدام طبقة تلافيفية أحادية البعد لاستخراج الميزات بدلاً من الاعتماد على تبعيات الزمنية لتصنيف البيانات.

من خلال عدة اختبارات، تم تعديل طبقة **GRU** إلى حجم 64، في حين تم تعديل الطبقة المقترحة (1-dCNN) بمجموعتين من الطبقات التلافيفية. تتكون كل مجموعة من 32 مرشحًا بحجم 3 وتشفيت بمقدار 2. تم إجراء اختيارات المعلمات هذه بناءً على التجارب والتحليلات المكثفة، بهدف أساسي هو تحقيق إمكانية تعميم متسقة وتخفيف التجهيز الزائد. توضح **GRU** المقترحة أداءً فائقًا من حيث نسبة الإشارة إلى الضوضاء (**SNR**).

تتفوق **GRU** المقترحة على نهج الذاكرة طويلة-قصيرة الامد( **LSTM**) بمقدار 2 ديسيبل وتتغلب على **LSTM** ثنائية الاتجاه (**BILSTM**) بمقدار 4 ديسيبل. علاوة على ذلك، تتفوق نهج **GRU** المقترح على الطرق التقليدية مثل الخطأ التربيعي الأقل (**LS**)، ومتوسط الخطأ التربيعي (**MMSE**)، والحد الأقصى لتقدير القناة (**ML**). من ناحية أخرى، يتفوق نهج (**1-dCNN**) المقترح على نهج **GRU** بمقدار 4 ديسيبل. تم اختبار كل من النهجين المقترحين في ظل سيناريوهات مختلفة عن طريق ضبط

المعلمات مثل البادئة الدورية (**CP**)، والموجة الحاملة الفرعية التجريبية، وزيادة عدد المسارات. في جميع الظروف المختلفة، يتفوق كلا النهجين باستمرار على أحدث الأساليب في مراجعة الأدبيات، مع تغلب نهج(**1-dCNN**) بشكل خاص على نهج **GRU** المقترح. تتناول هذه الأطروحة اختبار أوقات التدريب لمختلف انواع الشبكات العصبية، بما في ذلك **1-dCNN**، **GRU**، **LSTM**، و**BiLSTM**، على جهاز كمبيوتر مزود بوحدة معالجة مركزية Intel Core i5-7210M بسرعة 2.50 جيجا هرتز، ونواتين، ووحدة معالجة رسومات NVidia GeForce 630 خارجية مع ذاكرة 2 جيجا. توضح النتائج أن كلاً من GRU و1-dCNN يتفوقان على **LSTM** و**BiLSTM**، في حين أن وقت تدريب **1-dCNN** أسرع بنحو 4 دقائق من **GRU** .

وزارة التعليم العالي والبحث العلمي
جامعة بابـل / كلية الهندسة
قسم الهندسة الكهربائية

# تعزيز اكتشاف الاشارة في انظمة الوصول المتعددغير المتعامدة باستخدام التعلم العميق

رســـالـــــة
مقدمة الى كلية الهندسة في جامعة بابل
وهي جزء من متطلبات نيل درجة الماجستير في الهندسة/ الهندسة الكهربائية/اتصالات

من قبل
مُحَمَّد ناجح كاظم حمزة

اشـراف
الاستاذ الدكتور رائد سليم هاشم الموسوي

1445هـ 2023م